The Journal of Experimental Biology 200, 583–600 (1997)
Printed in Great Britain © The Company of Biologists Limited 1997
JEB0425

DRAGONFLY FLIGHT

III. LIFT AND POWER REQUIREMENTS

J. M. WAKELING* AND C. P. ELLINGTON
Department of Zoology, University of Cambridge, Downing Street, Cambridge CB2 3EJ, UK

Accepted 28 October 1996

Summary

A mean lift coefficient quasi-steady analysis has been applied to the free flight of the dragonfly *Sympetrum sanguineum* and the damselfly *Calopteryx splendens*. The analysis accommodated the yaw and accelerations involved in free flight. For any given velocity or resultant aerodynamic force (thrust), the damselfly mean lift coefficient was higher than that for the dragonfly because of its clap and fling. For both species, the maximum mean lift coefficient $\bar{C}_L$ was higher than the steady $C_{L,max}$. Both species aligned their strokes planes to be nearly normal to the thrust, a strategy that reduces the $\bar{C}_L$ required for flight and which is different from the previously published hovering and slow dragonfly flights with stroke planes steeply inclined to the horizontal. Owing to the relatively low costs of accelerating the wing, the aerodynamic power required for flight represents the mechanical power output from the muscles. The maximum muscle mass-specific power was estimated at 156 and 166 W kg^{-1} for *S. sanguineum* and *C. splendens*, respectively. Measurements of heat production immediately after flight resulted in mechanical efficiency estimates of 13 % and 9 % for *S. sanguineum* and *C. splendens* muscles, respectively.

Key words: dragonfly, damselfly, *Sympetrum sanguineum*, *Calopteryx splendens*, quasi-steady analysis, acceleration, power, efficiency.

Introduction

Insects are able to undergo a whole variety of flight manoeuvres, and they may use particular styles for different activities. Migration and foraging over substantial distances for food may entail flight at constant velocities; however, many styles of flight are of an unsteady nature. Accelerations are involved when pursuing prey and for the avoidance of predators, and erratic flight paths are used both for display and for escape. Previous studies of insect aerodynamics have used quasi-steady methods to analyse steady flight (Osborne, 1951; Jensen, 1956; Weis-Fogh, 1973; Ellington, 1984*a–d*; Dudley and Ellington, 1990; Cooper, 1993; Willmott, 1995). These studies have considered hovering flight, or flight that is constrained by wind-tunnels. More recently, Dudley and DeVries (1990) have analysed the free migratory flight of the moth *Urania fulgens*, but again the flights were assumed to be at a constant velocity. The limited range of flight styles considered may not be representative of insect flight in general. The present paper extends quasi-steady methods to consider the accelerated flight of the dragonfly *Sympetrum sanguineum* and the damselfly *Calopteryx splendens*.

Aerodynamic studies of dragonfly flight are confounded by the problem of two functional pairs of wings, with flow interactions between the fore- and hindwing pairs. These interactions result in dramatic changes in force production with only minor alterations in wing kinematics (Saharon and Luttges, 1988; Luttges, 1989). To simplify this problem, the effect of all four wings can be modelled as a single actuator disc. The mass flux of air in the far wake must be the reaction to the aerodynamic force acting on the dragonfly. The induced velocity of this air can thus be calculated from the swept area of the wings and aerodynamic force. This approach has previously been taken by Osborne (1951) and Norberg (1975). Previous insect studies have considered the major force to be vertical weight support and have thus made the simplifying assumptions that the induced velocity must also be vertical. For the flights considered here (Wakeling and Ellington, 1997*b*), the aerodynamic force has components to overcome weight support, acceleration and parasite drag. This aerodynamic force, thrust, is thus not necessarily vertical. An imaginary coordinate system is introduced to bring the ‘thrust’ vertical in accordance with the weight support from previous studies; however, the velocity is then inclined to the horizontal. A general form of the Rankine–Froude estimate of induced velocity (Stepniewski and Keys, 1984) is thus used to calculated induced velocity and power.

Profile power is calculated from the relative velocity of the

*Present address: Gatty Marine Laboratory, School of Biological and Medical Sciences, University of St Andrews, Fife KY16 8LB, UK (e-mail: jmw5@st-andrews.ac.uk).

wings. Wing motion is reconstructed both within the stroke plane and from its elevation from that plane. The nature of these accelerated flights results in significant asymmetries in the relative velocities between the left and right wings owing to yaw. Each wing was therefore analysed separately. Mean lift coefficients and profile powers are calculated assuming an appropriate value for the profile drag, which was taken from the lift and drag measurements in Wakeling and Ellington (1997*a*).

The net inertial power for an oscillating wing is zero becauses the energy required to accelerate the wing at the beginning of each half-stroke will be recovered during deceleration at the end of the half-stroke. The insect can usefully recover some of the inertial power from wing deceleration either by storing it in elastic structures in the thorax or by using it to overcome aerodynamic power costs. The inertial cost of accelerating the wings is usually greater than the aerodynamic power requirements (Ellington, 1984*d*). However, a special case for inertial power has recently been highlighted for cases where it is less than the aerodynamic power (Dickinson and Lighton, 1995). If there is no elastic storage, then inertial power recovered during wing deceleration can be totally used to help pay the aerodynamic power cost for that part of the stroke. The net mechanical power during the stroke thus becomes the aerodynamic power. If there is perfect elastic storage of inertial power, then the net mechanical power is similarly the aerodynamic power. Thus, if the inertial power is less than the aerodynamic power, the net mechanical power required from the flight muscles is simply the aerodynamic power regardless of the extent of elastic storage. This case has been shown for some butterflies (Dudley and DeVries, 1990) and some *Drosophila* species (Dickinson and Lighton, 1995). The relatively low wingbeat frequencies for the dragonflies and damselflies in the present study result in them also satisfying this special case where the mechanical power requirements from the muscles can be estimated independently of any assumption as to the degree of elastic energy return.

The power lost by the flight muscles as heat can be calculated from the thermal properties of dragonflies during flight. Corbet (1983) recognised that some dragonflies may thermoregulate, and distinguished between two behavioural types: 'fliers' and 'perchers'. Fliers typically spend most of their time on the wing and they can thermoregulate by shunting blood and thus heat between their thorax and abdomen. Perchers only make short flights to pursue prey, mates and rivals, and there is little evidence for physiologically facilitated heat transfer between the thorax and abdomen; instead, they thermoregulate by controlling their perching posture and flight duration (Heinrich and Casey, 1978; Heinrich, 1993). The dragonfly and damselfly in the present study, *S. sanguineum* and *C. splendens*, are both perchers. May (1976) has shown that for small dragonflies in general there is relatively little effect of blood shunting on the conductance, and so the difference in conductance between live and dead dragonflies is negligible.

During flight, the relative air flow increases the rate of convective cooling (Church, 1960*b*; Casey, 1976; May, 1976), and so the conductance values used for the calculation of heat production should be measured while the dragonfly is cooling in an air stream of an appropriate velocity. In the present study, the conductances are found by cooling experiments in the jet of a wind-tunnel. These are used, in conjunction with measurements of thoracic temperatures immediately after flight, to estimate the power lost as heat from the thoracic muscles. Muscle mechanical efficiencies are calculated for these dragonfly flights from the aerodynamic estimates of the mechanical power requirements, coupled to the measurements of heat production during flight.

Materials and methods

Lift and drag data for both the bodies and wings of the dragonfly *Sympetrum sanguineum* (Müller) and the damselfly *Calopteryx splendens* (Harris) were taken from Wakeling and Ellington (1997*a*), and kinematic data for their flights were taken from Wakeling and Ellington (1997*b*). The velocity and acceleration are assumed to be constant for the duration of each wingbeat analysed. A detailed description of the morphological parameters for these and a further five dragonfly species is available elsewhere (Wakeling, 1997) but the parameters relevent to this paper are given in Table 1 and follow the notation in Ellington (1984*a*). Data were processed in Mathematica and MathCad routines on a Macintosh Quadra 650 computer. All calculations assumed values of $\rho=1.165\,\mathrm{kg\,m^{-3}}$ for the air density and $\nu=1.608\times10^{-5}\,\mathrm{m^2\,s^{-1}}$ for the kinematic viscosity, which are appropriate to the 30 °C flight conditions.

Power terms are calculated as power P (mW) and muscle mass-specific power P^* ($\mathrm{W\,kg^{-1}}$), which is power per unit thoracic muscle mass. The term 'thrust', T, refers to the total aerodynamic force (as in Wakeling and Ellington, 1997*b*), and this is not necessarily horizontal or vertical.

Parasite power

Parasite power P_{par} is expended to overcome the parasite drag on the dragonfly body. The force required to overcome parasite drag D_{par} comes from the thrust generated by the wings, and thus parasite power is implicitly included in the induced power when this is derived from the total thrust.

Studies of insect flight have traditionally divided the total thrust into vertical and horizontal components, which respectively balance the insect's weight and parasite drag. This is a convenient division because D_{par} is typically much smaller than the weight, and it can be estimated independently. Parasite power is then simply given by:

$$P_{\mathrm{par}} = VD_{\mathrm{par}}\,. \qquad (1)$$

The overall thrust is nearly vertical, as required by the dominating role of weight support, so the induced velocity V is also approximately vertical. The induced power P_{ind} is conventionally calculated as if it is indeed vertical, and thus P_{ind} represents the kinetic energy imparted to the air solely for

Table 1. *Morphological parameters used for the power calculations*

		Forewings								Hindwings							
Flight	m (mg)	R (mm)	S (mm^2)	$\hat{r}_1(S)$	$\hat{r}_2(S)$	$\hat{v}$	$\hat{r}_2(v)$	$\hat{h}$ (%)	$\hat{r}_2(m)$	R (mm)	S (mm^2)	$\hat{r}_1(S)$	$\hat{r}_2(S)$	$\hat{v}$	$\hat{r}_2(v)$	$\hat{h}$ (%)	$\hat{r}_2(m)$
SSan2	121.9	27.85	327.87	0.507	0.570	1.048	0.567	0.0126	0.538	26.90	413.45	0.446	0.520	1.052	0.478	0.0124	0.495
SSan5	133.0	27.23	312.38	0.513	0.574	1.060	0.574	0.0141	0.565	26.17	400.96	0.447	0.521	1.050	0.481	0.0129	0.490
SSan6	111.5	26.38	292.59	0.507	0.570	1.047	0.568	0.0138	0.537	25.49	380.01	0.453	0.525	1.050	0.489	0.0137	0.499
SSan9	139.3	29.44	357.44	0.507	0.570	1.050	0.568	0.0124	0.519	28.54	460.24	0.444	0.519	1.054	0.476	0.0123	0.481
CS1	91.0	30.43	434.71	0.548	0.601	1.113	0.613	0.0115	0.502	29.36	381.95	0.565	0.613	1.159	0.628	0.0135	0.490
CS2	93.6	29.44	400.51	0.553	0.604	1.126	0.617	0.0115	0.489	28.77	387.11	0.553	0.604	1.118	0.618	0.0124	0.508
CS3	123.6	30.42	427.32	0.552	0.603	1.123	0.616	0.0120	0.478	29.28	406.92	0.551	0.603	1.119	0.615	0.0112	0.511
CS4	119.1	29.68	398.05	0.557	0.607	1.132	0.623	0.0117	0.510	29.14	380.53	0.557	0.607	1.126	0.622	0.0125	0.500

SSan, *Sympetrum sanguineum*; CS, *Calopteryx splendens*.

m, total mass; R, wing length; S, combined area of left and right wings; $\hat{r}_1(S)$ and $\hat{r}_2(S)$, first and second radii of wing area; $\hat{r}_2(v)$ and $\hat{r}_2(m)$, second radii of wing virtual mass and mass; $\hat{v}$, non-dimensional virtual mass of wing pair; $\hat{h}$ (%), mean wing thickness/wing length.

Full details of these parameters can be found in Ellington (1984*a*).

Table 2. *Flight parameters in thrust-based coordinates and other parameters used in the quasi-steady calculations*

Flight	m (mg)	V ($m\,s^{-1}$)	$\hat{T}$	$-\alpha'$ (degrees)	w ($m\,s^{-1}$)	β'_f (degrees)	β'_h (degrees)	A_{Zf}	B_{Zf}	A_{Zh}	B_{Zh}	$\hat{T}_f$	$\bar{C}_L$
SSan2.1	121.9	1.657	1.65	66.75	0.425	8.36	9.35	0.561	–0.538	0.643	–0.660	0.470	1.03
SSan2.3	121.9	1.053	1.15	72.41	0.398	6.86	7.11	0.737	–0.501	0.579	–0.522	0.574	0.92
SSan5.1	133.0	1.519	2.65	24.14	0.736	–7.59	–2.72	0.207	–0.178	0.386	–0.234	0.342	1.83
SSan5.2	133.0	0.698	0.85	50.73	0.507	2.82	8.27	0.441	–0.315	0.805	–0.406	0.342	0.92
SSan6.1	111.5	1.463	2.16	75.79	0.532	–17.65	–17.61	0.536	–0.423	0.681	–0.536	0.441	0.98
SSan6.2	111.5	1.525	1.41	65.54	0.369	–10.51	–12.35	0.621	–0.515	0.845	–0.630	0.418	0.84
SSan9.1	139.3	1.271	1.26	83.88	0.409	–5.45	–3.08	0.615	–0.516	0.662	–0.615	0.488	0.96
CS1.1	91.0	0.673	1.24	31.40	0.367	–3.68	3.13	0.655	–0.313	0.494	–0.221	0.568	0.96
CS1.3	91.0	0.540	1.42	56.47	0.419	11.29	20.91	0.424	–0.271	0.364	–0.219	0.537	1.39
CS2.2	93.6	1.036	1.56	48.09	0.529	–4.89	–0.10	0.367	–0.379	0.377	–0.396	0.494	1.55
CS2.3	93.6	1.161	1.22	86.68	0.310	–7.76	–4.52	1.070	–0.739	0.610	–0.607	0.660	0.76
CS2.5	93.6	0.555	1.28	45.79	0.532	–5.61	7.20	0.430	–0.322	0.518	–0.306	0.446	1.19
CS3.2	123.6	1.430	1.30	48.93	0.252	17.13	28.31	0.656	–0.553	0.648	–0.565	0.505	0.94
CS3.3	123.6	0.936	0.79	27.31	0.229	18.88	46.39	0.611	–0.430	0.347	–0.271	0.641	1.19
CS3.5	123.6	1.661	1.59	69.56	0.259	–12.59	–2.41	0.674	–0.599	0.785	–0.666	0.459	0.86
CS4.2	119.1	0.494	1.27	59.56	0.556	-6.38	7.47	0.397	–0.267	0.472	–0.279	0.453	1.28

Symbols are defined in the text.

SSan, *Sympetrum sanguineum*; CS, *Calopteryx splendens*.

Lift coefficients are calculated assuming $C_{D,pro}$=0.2 and lift is generated on both up- and downstrokes.

weight support. The kinetic energy imparted by the horizontal force component is ignored, because it is treated independently by the D_{par} calculation, but it must be realised that the induced velocity has a horizontal as well as a vertical component. Where D_{par} is large, for instance at fast flight speeds or where there are large horizontal accelerations, the induced velocity may differ significantly in magnitude and direction from the traditional estimate based on weight support alone. This will lead to errors, albeit probably small, in estimates of both the angles of incidence and the profile drag of the wings. Because of the accelerating flights in this study, the induced velocity was calculated from the total thrust; P_{par} is therefore implicitly included in P_{ind}.

Induced power and induced velocity

To calculate induced power, the induced velocity resulting from total thrust production must first be calculated. Thrust is the vector sum of the weight support, the parasite drag, body lift and any unbalanced force that accelerates the dragonfly:

$$\boldsymbol{T} = m\boldsymbol{a} - m\boldsymbol{g} - \boldsymbol{D}_{\mathbf{par}} - \boldsymbol{L}_{\mathbf{par}}, \quad (2)$$

where m is body mass, $\boldsymbol{g}$ is the acceleration due to gravity and $\boldsymbol{a}$ is acceleration. Preliminary calculations showed the lift generated by the dragonfly body, L_{par}, to be less that 1 % of the total thrust, and so it was ignored in the present study. This thrust implicitly includes the acceleration and drag components of the body, and so the induced power estimates also include the power required to accelerate the body and overcome parasite drag.

To bring this thrust more in line with the weight support that is conventionally used for induced velocity calculations, the dragonfly coordinate system was transformed to a thrust-based X,Y,Z coordinate system where the thrust is vertical along the Z axis, and the X axis is parallel to the sagittal plane (Fig. 1). This thrust-based system is similar to the conventional gravitational coordinate system except that the 'vertical' force equals the thrust instead of the weight. The non-dimensional thrust $\hat{T}$ expresses total aerodynamic force as a proportion of the weight:

$$\hat{T} = \frac{T}{m\boldsymbol{g}} . \quad (3)$$

Roll angles, which had reached 58 ° in the horizontal x',y',z' coordinates (Wakeling and Ellington, 1997*b*), take values of less than 12 ° in thrust-based coordinates for all except one of the flights in the present study; these angles are more typical of results for insects flying at constant horizontal velocities in a wind-tunnel.

The actuator disc is, by definition, 'horizontal' in the thrust-based coordinates. It represents the area over which the wings interact with the air to give it a 'downwards' impulse and thus can be considered as the projection of the swept area of the wings onto the X,Y plane. This actuator disc is nearly parallel to the stroke plane, which is approximately normal to the thrust (see Wakeling and Ellington, 1997*b*), so the actuator disc is

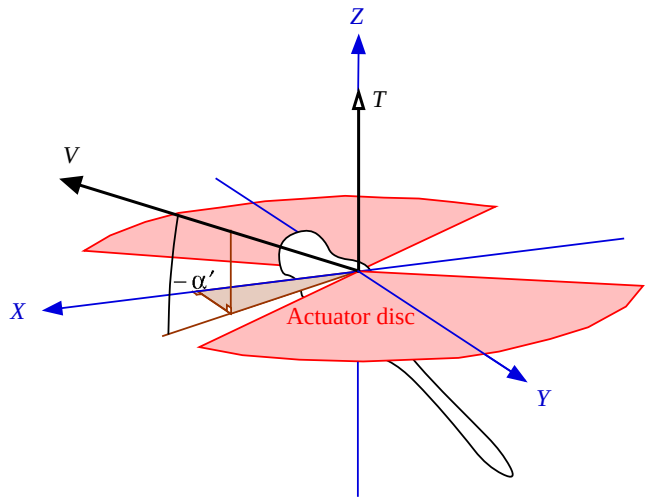

Fig. 1. In the thrust-based coordinate system, the thrust T is 'vertical' along the Z axis, and the dragonfly faces along the X axis. The forward velocity V is inclined by $-\alpha'$ to the horizontal actuator disc in the X,Y plane.

taken to have an area $A_0=\Phi R^2$, where Φ is stroke amplitude and R is wing length. This estimation of actuator disc area is never more than 6 % greater than the equivalent areas $\Phi R^2\cos\beta$, where β is the stroke plane angle, used by Ellington (1984*b*), Ennos (1989) and Dudley and Ellington (1990).

The induced velocity was calculated from the mass flux of air that must be moved by the actuator disc to balance the thrust. The induced velocity w for the general case of a rotor with velocity V which is inclined at an angle $-\alpha'$ to the actuator disc is:

$$w^4 - 2Vw^3\sin\alpha' + V^2w^2 - \left(\frac{T}{2\rho A_0}\right)^2 = 0 \quad (4)$$

(Stepniewski and Keys, 1984, equation 2.32). It proves convenient to normalise this equation using the Rankine–Froude estimate of induced velocity w_0 required for hovering with $T=m\boldsymbol{g}$:

$$w_0 = \sqrt{\frac{m\boldsymbol{g}}{2\rho A_0}} . \quad (5)$$

Equation 4 can then be written in terms of a non-dimensional velocity V' ($=V/w_0$) and induced velocity $\hat{w}$ ($=w/w_0$) to give:

$$\frac{1}{\hat{T}^2 k_{ind}^4}\{\hat{w}^4 - 2V'\hat{w}^3\sin\alpha' + V'^2\hat{w}^2 - 1\} = 0 . \quad (6)$$

The induced velocity factor k_{ind} has been added to this equation to correct for the tip losses and non-uniform flow across the actuator disc. Pennycuick (1975) suggests that a value of k_{ind}=1.2 is appropriate for animal flight, and this has been confirmed for hovering flight with horizontal stroke planes using vortex theories (Ellington, 1984*c*). k_{ind} should be lower for two pairs of wings having reduced wake periodicity and thus tip losses, but higher for slight inclinations of the stroke

planes (Ellington 1984*c*); the value of k_{ind}=1.2 is probably reasonable for dragonflies and has been used in the present study in the absence of a better estimate.

The flights in the present study took values of $-87° < \alpha' < -24°$, and so equations 4 and 6 have been used throughout. Equation 4, however, has two limiting conditions which can be further simplified. The case where $\alpha'=0°$ describes an actuator disc moving parallel to its plane, and is given in a normalised form by:

$$\hat{w}_{(\alpha'=0°)} = \sqrt{-0.5V'^2 + \sqrt{0.25V'^4 + 1}}\,. \qquad (7)$$

This condition is appropriate for horizontal flights at constant velocity, and has been used by Osborne (1951), Dudley and Ellington (1990) and Cooper (1993). The second case, where $\alpha'=-90°$, is for hovering or vertical climbing flight with the velocity perpendicular to the actuator disc and is expressed in non-dimensional form by:

$$\hat{w}_{(\alpha'=-90°)} = -0.5V' + \sqrt{0.25V'^2 + 1}\,; \qquad (8)$$

this has been used for the slow climbing flight of *Sympetrum frequens* (Azuma *et al.* 1985).

Induced power P_{ind} is given by the product of thrust and the velocity through the actuator disc:

$$P_{ind} = T(w - V\sin\alpha')\,. \qquad (9)$$

The quasi-steady model: force coefficients and profile power

Quasi-steady aerodynamic forces depend on the relative velocity of the wings, and this must first be calculated before the force coefficients and profile power are estimated.

This analysis is based on a quasi-steady model developed by C. P. Ellington (unpublished) for steady, level flight without yaw. Ellington assumed a sinusoidal wing motion confined to the stroke plane. Dragonfly wingbeats are neither sinusoidal nor are they restricted to movement in a single plane (see Wakeling and Ellington, 1997*b*). Ellington's analysis has therefore been modified to include the precise motion of the wing both in the stroke plane and its elevation away from that plane. Yaw has also been added to this model, leading to the profile power costs being asymmetrical between the left and right wings. Profile power is thus calculated for each individual wing for the dragonflies.

The stroke angle ϕ of the wing within the stroke plane and the angle of elevation θ above the stroke plane are calculated using equation 12 and data from Tables 2 and 3 in Wakeling and Ellington (1997*b*), using the first four harmonics of each Fourier series. Non-dimensional forms of the angular velocities are given by:

$$\dot{\hat{\phi}} = \frac{2\dot{\phi}}{n\Phi} \qquad (10a)$$

and

$$\dot{\hat{\theta}} = \frac{2\dot{\theta}}{n\Phi}\,, \qquad (10b)$$

where n is the wingbeat frequency, Φ is the stroke amplitude and a dot above a symbol denotes differentiation with respect to time. Velocities are normalised to the mean flapping velocity of the wingtip U_t (=2ΦnR).

When the angle between the stroke plane and the X,Y plane is β', the non-dimensional flapping velocity of the wing $\hat{U}$ is given by:

$$\hat{U} = \frac{\hat{r}\dot{\hat{\phi}}}{4}\begin{pmatrix}\cos\beta'\cos\phi\\ \sin\phi\\ -\sin\beta'\cos\phi\end{pmatrix} + \frac{\hat{r}\dot{\hat{\theta}}}{4}\begin{pmatrix}\sin\beta'\\ 0\\ \cos\beta'\end{pmatrix}, \qquad (11)$$

where $\hat{r}$ is the non-dimensional radial position along the wing (r/R).

The relative flight velocity is the sum of the forward and induced velocities and is expressed by the normalised velocity $\hat{J}$, where:

$$\begin{pmatrix}\hat{J}_X\\ \hat{J}_Y\\ \hat{J}_Z\end{pmatrix} = \frac{1}{U_t}\begin{pmatrix}V_X\\ \pm V_Y\\ V_Z + w\end{pmatrix}. \qquad (12)$$

$\hat{J}$ is a form of the advance ratio which also includes the induced velocity. Positive values are taken by V_X and V_Z for forward and upward flight. To account for yaw, the sign of V_Y is opposite for calculations of the relative velocity for the left and right wings. For flight with no yaw, V_Y is zero. The calculations in the present study are unusual in that the effects of V_Y are considered. Yaw has been ignored in all previous aerodynamic studies on insect flight, but the dragonflies in thrust-based coordinates show yaws of up to 56°. Ignoring V_Y here would overestimate $\bar{C}_L$ by up to 6% and underestimate P_{pro} by up to 17%. V_Y thus makes significant contributions to the force balance and power terms, and so is included in these calculations.

The relative velocity of the wing is the vector sum of the flapping velocity $\hat{U}$ and the relative flight velocity $\hat{J}$. Any spanwise component of this relative velocity is neglected in a quasi-steady analysis, because it is thought to have little effect on the aerodynamic forces. The non-dimensional relative velocity ignoring the spanwise component, $\hat{U}_r$, has magnitude:

$$\hat{U}_r = \left[\left(\frac{-\hat{r}\dot{\hat{\theta}}}{4} - \hat{J}_X\sin\beta' - \hat{J}_Z\cos\beta'\right)^2 + \left(\frac{\hat{r}\dot{\hat{\phi}}}{4} - \hat{J}_X\cos\beta'\cos\phi - \hat{J}_Y\sin\phi + \hat{J}_Z\cos\phi\sin\beta'\right)^2\right]^{\frac{1}{2}}. \qquad (13)$$

Direction numbers for $\hat{U}_r$, the 'drag' components, are given by λ_D, μ_D and ν_D, respectively, for the X, Y and Z directions. These direction numbers are equal to the direction cosines multiplied by $\hat{U}_r$:

$$\lambda_D = -0.25\hat{r}(\dot{\hat{\theta}}\sin\beta' - \dot{\hat{\phi}}\cos\beta'\cos\phi) - \hat{J}_X(1-\cos^2\beta'\sin^2\phi) - \hat{J}_Y\cos\beta'\cos\phi\sin\phi - \hat{J}_Z\cos\beta'\sin\beta'\sin^2\phi\,, \qquad (14)$$

$$\mu_D = 0.25\hat{r}\dot{\hat{\phi}}\sin\phi - \hat{J}_X\cos\beta'\cos\phi\sin\phi - \hat{J}_Y\sin^2\phi + \hat{J}_Z\sin\beta'\cos\phi\sin\phi\,, \qquad (15)$$

$$\nu_D = -0.25\hat{r}(\dot{\hat{\phi}}\cos\phi\sin\beta' + \dot{\hat{\theta}}\cos\beta') - \hat{J}_X\cos\beta'\sin\beta'\sin^2\phi + \hat{J}_Y\cos\phi\sin\beta'\sin\phi - \hat{J}_Z(1-\sin^2\beta'\sin^2\phi). \quad (16)$$

Similar direction numbers, normal to $\hat{U}_r$, are resolved for 'lift' and take the subscript L:

$$\lambda_L = -0.25\hat{r}\dot{\hat{\phi}}\sin\beta' - 0.25\hat{r}\dot{\hat{\theta}}\cos\beta'\cos\phi + \hat{J}_Y\sin\beta'\sin\phi - \hat{J}_Z\cos\phi, \quad (17)$$

$$\mu_L = -0.25\hat{r}\dot{\hat{\theta}}\sin\phi - \hat{J}_X\sin\beta'\sin\phi - \hat{J}_Z\cos\beta'\sin\phi, \quad (18)$$

$$\nu_L = -0.25\hat{r}\dot{\hat{\phi}}\cos\beta' + 0.25\hat{r}\dot{\hat{\theta}}\cos\phi\sin\beta' + \hat{J}_X\cos\phi + \hat{J}_Y\cos\beta'\sin\phi. \quad (19)$$

As an intermediate step in calculating the mean aerodynamic forces, non-dimensional integrals sum the velocity components throughout the stroke for all chordwise elements of the wing. Taking a non-dimensional wingbeat period $0<\hat{t}<1$, and the downstroke and upstroke periods as $\hat{t}_d$ and $\hat{t}_u$, respectively, the integrals to describe the drag components in the *Z* direction are given by:

$$I_{D,Z(d)} = \int_{\hat{t}_d}\int_{\hat{r}} \hat{c}\nu_D\hat{U}_r\mathrm{d}\hat{r}\mathrm{d}\hat{t}, \quad (20a)$$

and

$$I_{D,Z(u)} = \int_{\hat{t}_u}\int_{\hat{r}} \hat{c}\nu_D\hat{U}_r\mathrm{d}\hat{r}\mathrm{d}\hat{t}, \quad (20b)$$

where $\hat{c}$ is the non-dimensional chord as calculated from $\hat{r}_1(S)$ and $\hat{r}_2(S)$ (the first and second radii of wing area) using a Beta function (Ellington, 1984*a*) and the subscripts d and u denote downstroke and upstroke, respectively. Similar integrals can be constructed for the drag components along the *X* and *Y* directions, and also for all three lift components. The integrals are additionally given subscripts D or L depending on whether they are used for drag of lift calculations, respectively. Values for the 'lift' integrals are positive if the relative velocity hits the ventral surface of the wing and negative for the dorsal surface, i.e. positive for the downstroke and negative for the upstroke when the wing flips over. The factor ζ is then used to convert these integrals to force coefficients relative to the non-dimensional thrust $\hat{T}$:

$$\zeta = \frac{\rho S U_t^2}{2\hat{T}m\boldsymbol{g}}, \quad (21)$$

where *S* is the wing area. Wing areas given in Table 1 are for wing pairs, however, for yawed flight where the forces on the left and right wings are calculated separately and so the appropriate value of *S* for a single wing must be used.

Lift and drag contributions to the normalised force in the *Z* direction, A_Z and B_Z, respectively, are given by:

$$A_Z = \zeta(\hat{t}_d I_{L,Z(d)} - \hat{t}_u I_{L,Z(u)}) \quad (22a)$$

and

$$B_Z = \zeta(\hat{t}_d I_{D,Z(d)} + \hat{t}_u I_{D,Z(u)}). \quad (22b)$$

The forces can then be solved for the quasi-steady analysis; the force in the *Z* direction (both lift and drag) must match the thrust, which by definition is also in the *Z* direction. This quasi-steady solution is:

$$A_Z C_L + B_Z C_{D,pro} = 1. \quad (23)$$

Where the profile drag coefficient $C_{D,pro}$ can be estimated, this equation can be solved for a mean lift coefficient $\bar{C}_L$ at which the wings must be operating throughout their stroke to generate the required total thrust. Dragonflies have two pairs of wings, however, and each wing pair supports only a fraction of the total thrust. If a single value of $\bar{C}_L$ is assumed for both wing pairs, the forewings generate a fraction $\hat{T}_f$ of the total thrust:

$$\hat{T}_f = \frac{A_{Zh}B_{Zf}C_{D,pro} + A_{Zf}(1 - B_{Zh}C_{D,pro})}{A_{Zf} + A_{Zh}}, \quad (24)$$

where subscripts f and h denote the fore- and hindwings, respectively. As with C_L, a common value of $C_{D,pro}$ is assumed for both wing pairs. The minimum $\bar{C}_L$ at which both wings must operate throughout their stroke to support *T* is then given by:

$$\bar{C}_L = \frac{\hat{T}_f - B_{Zf}C_{D,pro}}{A_{Zf}}. \quad (25)$$

Profile power is similarly calculated from non-dimensional integrals that describe the cube of $\hat{U}_r$ throughout the wingstroke. These integrals for the downstroke and the upstroke are:

$$I_{P(d)} = \int_{\hat{t}_d}\int_{\hat{r}} \hat{c}\hat{U}_r^3\mathrm{d}\hat{r}\mathrm{d}\hat{t}, \quad (26a)$$

and

$$I_{P(u)} = \int_{\hat{t}_u}\int_{\hat{r}} \hat{c}\hat{U}_r^3\mathrm{d}\hat{r}\mathrm{d}\hat{t}. \quad (26b)$$

The power factor σ gives dimensions to these integrals, and is:

$$\sigma = 0.5\rho S U_t^3(\hat{t}_d I_{P(d)} + \hat{t}_u I_{P(u)}). \quad (27)$$

The profile power costs for each wing pair are then given by:

$$P_{pro} = \sigma C_{D,pro}. \quad (28)$$

As can be seen from equations 25 and 28, the estimates of both $\bar{C}_L$ and P_{pro} are dependent on the choice of $C_{D,pro}$. The force measurements from Wakeling and Ellington (1997*a*) showed that the minimum values for $C_{D,pro}$ are, on average, 0.13 for *S. sanguineum* wings and 0.10 for *C. splendens* wings. These values are for a zero angle of incidence and comprise virtually all skin friction. However, when the wings operate at a non-zero angle of incidence, the pressure drag component of $C_{D,pro}$ increases. Data from Azuma *et al.* (1985) show that the mean angle of incidence for *Sympetrum frequens* during slow climbing flight was 26 °, and data from Rüppell (1989) suggest a mean value of 22 ° for *C. splendens* during a variety of flights. The profile drag estimates must thus include the pressure drag component for non-zero angles of incidence.

Within the range of angle of attack α with linearly increasing C_L, the drag coefficient follows the parabolic law:

$$C_D = C_{D,pro} + \frac{C_L^2}{b} , \quad (29)$$

(von Mises, 1959) where b is a constant and C_L^2/b is the coefficient of induced drag. This induced drag coefficient was calculated for each of the four types of wing from Wakeling and Ellington (1997*a*) in the linear range of C_L for $0°<\alpha<20°$ and was subtracted from C_D to obtain $C_{D,pro}$ (equation 29). $C_{D,pro}$ was then estimated from linear regression of $C_{D,pro}$ with α. Assuming mean angles of incidence of 26° and 22°, the mean values are $C_{D,pro}\approx0.20$ for *S. sanguineum* and $C_{D,pro}\approx0.17$ for *C. splendens*.

Ellington (1984*d*) suggests that for the large angles of incidence used for hovering, $C_{D,pro}$ tends to vary inversely with the square root of Reynolds number *Re* and is:

$$C_{D,pro} \approx \frac{7}{\sqrt{Re}} . \quad (30)$$

However, these dragonflies were not hovering, and their angles of attack are smaller than those typical of hovering insects (Ellington, 1984*b*). The relationship of equation 30 will therefore be used as an upper estimate for $C_{D,pro}$ for these dragonflies.

The non-dimensional integrals in equation 26 give the cube of the normalised relative velocity, and these can be used for calculating a mean Reynolds number for use in equation 30:

$$Re = U_t^3 \sqrt{\hat{t}_d I_{P(d)} + \hat{t}_u I_{P(u)}} \; \frac{2R}{AR\nu} , \quad (31)$$

where AR is the aspect ratio and ν is the kinematic viscosity of air. Profile drag values appropriate to the present study according to equations 30 and 31 are $C_{D,pro}\approx0.20$ for *S. sanguineum* and $C_{D,pro}\approx0.23$ for *C. splendens*.

Estimates of $C_{D,pro}$ are remarkably similar for the two methods, and a mean profile drag coefficient of 0.20 was therefore chosen for all the flights in the present study. It should be noted that this $C_{D,pro}$ is derived from steady-state measurements (Wakeling and Ellington, 1997*a*); however, it is used to estimate what are ultimately unsteady values for $\bar{C}_L$. At the Reynolds number and angle of attack used by the odonates, the profile drag is dominated by pressure drag. Unsteady mechanisms that increase the amount of circulation generated by the wings should increase drag as well as lift since the total pressure force on a thin wing must be roughly normal to the surface of that wing. The steady-state estimates for $C_{D,pro}$ probably represent a lower limit of those that occur during flight and will thus result in conservative estimates for $\bar{C}_L$ and P_{pro}. When better estimates for $C_{D,pro}$ become available, then $\bar{C}_L$ and P_{pro} can be easily recalculated using equations 25 and 28.

Profile drag and wake inefficiencies

Owing to the geometry of the wing motion, there is a small

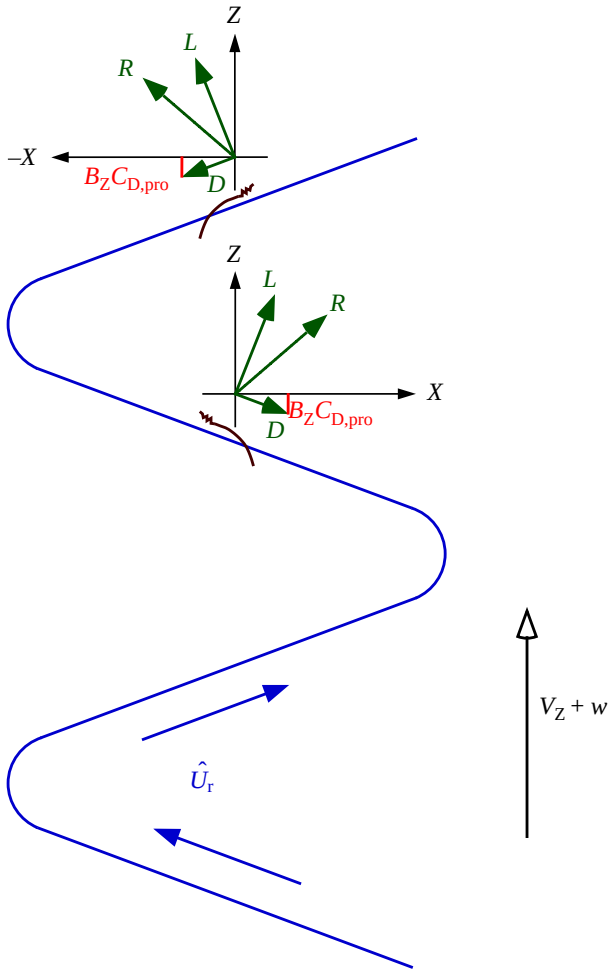

Fig. 2. A ‘vertical’ component of profile drag, $B_ZC_{D,pro}$, acts ‘downwards’ during both the morphological up- and downstrokes. The path of the wingtip, moving at velocity $\hat{U}_r$, is drawn in blue. Wing profiles are superimposed on this path, with lift L and drag D forces appropriate to those positions. The ‘downwards’ $B_ZC_{D,pro}$ is indicated by the red bar for each half-stroke. R, resultant force; X and Z, directions in the X,Y,Z coordinate system; V_Z, velocity in the Z direction; w, induced velocity.

‘downwards’ component to the profile drag $B_ZC_{D,pro}$ (equation 23) during both the morphological up- and downstrokes (Fig. 2). The ‘downwards’ nature of this force is indicated by B_Z taking a negative sign. This force is caused by air being dragged ‘upwards’ with the wing owing to the ‘upward’ component of $\hat{U}_r$, and so it corresponds to a small upwash imparted to the wake as a result of profile drag.

The power cost of creating the upwash by $B_ZC_{D,pro}$ is implicitly included in the P_{pro} estimate. However, a downwash must be generated to cancel this upwash, in addition to the net downwash to provide thrust support. Extra energy must thus be imparted into the momentum jet which does not appear as net momentum in the far wake; this is an inefficiency in the momentum jet due to the ‘vertical’ component of profile drag opposing the thrust of the jet.

The induced power calculations from equations 2–9

balanced the momentum flux in the far wake to the net thrust. The thrust, however, must be augmented by the vertical component of D_{pro}; this augmented thrust, $\hat{T}'$, is given by:

$$\hat{T}' = \hat{T}\{1-[\hat{T}_f B_{Zf}\bar{C}_{D,pro} + (1-\hat{T}_f)B_{Zh}\bar{C}_{D,pro}]\}. \quad (32)$$

$\hat{T}'$ is, on average, 12 % greater than $\hat{T}$. A revised estimate for induced power, P_{ind}', including the power required for these inefficiencies in the wake, can thus be calculated using equation 6 with $\hat{T}'$ to calculate a corresponding value for the induced velocity w'. P_{ind}' is then calculated from equation 9 with $T=\hat{T}'m\boldsymbol{g}$ and the new induced velocity w'.

In helicopter flight, the vertical component of profile drag on the rotors is negligible compared with the induced drag, and thus the profile drag contribution to the downwash is also negligible and is ignored. Animal flight studies have drawn their methods from the aeronautics literature and so have also ignored this component. Profile power forms a larger fraction of the mechanical power requirements of animal flight (Ellington, 1991). Dragonflies are unusual animal fliers in that they have two functional pairs of wings; dragonfly profile power is typically 75 % of the induced power, and so the contribution of $B_Z C_{D,pro}$ to the momentum jet may be even greater than for other animals.

The correction for these wake inefficiencies typically increases the total power requirements by 6 % and so constitutes a significant improvement to the power estimates for dragonflies. Values for P_{pro} and P_{ind} are presented for comparison with previous studies. The aerodynamic power P_{aero} is the sum of these two powers, but additionally includes this correction to include the wake inefficiency:

$$P_{aero} = P_{ind}' + P_{pro}. \quad (33)$$

For cases where there is a net 'upward' component to the profile drag, this drag contributes usefully to the momentum jet. The induced thrust required from the momentum jet is thus reduced by $B_Z C_{D,pro}$, with a corresponding reduction in the induced power requirements. The take-off flight of the large cabbage white butterfly *Pieris brassicae* shows such a net upward component to its profile drag (Ellington, 1980). Its stroke plane is approximately vertical, and the wings are moved with the chord perpendicular to the motion during the downstroke; during the upstroke, the wings are strongly supinated, producing an angle of attack near zero. Vertical stroke plane flights have been recorded in other butterflies (Betts and Wootton, 1986; Sunada *et al.* 1993). Similar kinematics are also seen in G. Rüppell's films of damselfly flight; during strong backwards accelerations, the damselflies can use a synchronous 'downstroke', using large angles of attack, to squeeze air forwards and generate profile drag in a direction useful for their flight.

Inertial power

The inertial power P_{acc} required to accelerate the mass of a wing pair and the added mass of air that moves with it is given by the angular velocity of the wing multiplied by the inertial torque I_w, where I_w is the moment of inertia of the wing pair and the added mass (Ellington, 1984*d*). The mean P_{acc} is equal to the kinetic energy gained by the wing pair, $0.5I_w\dot{\phi}_{max}^2$, divided by the period $1/4n$ of acceleration, and is equal to $2nI_w\dot{\phi}_{max}^2$.

This approach has been used by Ellington (1984*d*), Dudley and Ellington (1990) and Cooper (1993), with the assumption that the wings oscillate with a simple harmonic motion. Dragonflies do not fit this assumption (Wakeling and Ellington, 1997*b*), which would lead to errors in the estimate for $\dot{\phi}_{max}$. Simple harmonic motion would underestimate $\dot{\phi}_{max}$ for flight CS3.3 where the wings were held virtually motionless for a period at their most dorsal position and then moved relatively quickly during the downstroke; it would also overestimate $\dot{\phi}_{max}$ for cases such as CS2.3, where the angular velocity is reasonably constant throughout the upstroke and the downstroke. For wingbeats where the downstroke-to-upstroke ratio is significantly different from 1, such as CS1.3, the maximum angular velocity will be different for each half-stroke and so must be calculated separately.

The angular wing velocity was calculated from its components both within the stroke plane $\dot{\phi}$ and away from the stroke plane $\dot{\phi}$. P_{acc} is thus given by:

$$P_{acc} = nI_w[(\dot{\phi}^2+\dot{\theta}^2)_{u_{max}} + (\dot{\phi}^2+\dot{\theta}^2)_{d_{max}}], \quad (34)$$

where the subscripts u and d denote values for the upstroke and downstroke, respectively. I_w is equal to:

$$I_w = \rho_w S R^3 \hat{h}\hat{r}_2^2(m) + \frac{\pi\rho S^2 R\hat{v}\hat{r}_2^2(v)}{8}, \quad (35)$$

where $\hat{h}$ is the non-dimensional mean wing thickness (Dudley and Ellington, 1990), using the wing parameters $\hat{r}_1(m)$ and $\hat{r}_2(v)$ from Table 1 and the wing density ρ_w taken as $1200\,kg\,m^{-3}$, the density of solid cuticle (Wainright *et al.* 1976).

The contribution of inertial power to the overall costs of flight will be discussed below in connection with the efficiencies of flight.

Heat production

Owing to inefficiencies in the flight musculature, most of the power expended by the muscles is lost as heat. This power loss can be estimated from measurements of the thermal conductance of the thorax and the thoracic temperature elevation above ambient.

Flight temperatures were measured for *S. sanguineum* and *C. splendens* in the flight enclosure described in Wakeling and Ellington (1997*a*). The dragonflies were encouraged to make ten consecutive flights around the enclosure; each flight consisted of flying one or more lengths of the enclosure and was stimulated by gently squeezing the abdomens of perching dragonflies. Immediately after a dragonfly had finished its ten flights, a thermocouple was inserted laterally into its thorax between the metathoracic and mesothoracic segments. These type K thermocouples were constructed from 0.125 mm wires, joined by silver solder and bonded to the end of a sharp wooden

rod with epoxy resin; temperatures were read from an RS 611-234 temperature meter. Weis-Fogh (1964) has shown that the thoracic temperature of the locust, a larger insect than these dragonflies and thus having a greater thermal inertia, rises to a near-maximal value within 2 min of the initiation of flight; the temperatures measured here will similarly be close to maximum. Ambient temperature was measured using a second thermocouple in an open shaded box in the enclosure. Individuals underwent this flight and temperature recording procedure no more than four times, and they were then killed with ethyl acetate vapour, and weighed.

Two sets of conductance measurements were made for each of four individuals each of *S. sanguineum* and *C. splendens*. These insects were killed with ethyl acetate vapour, and their bodies were aligned with the flow of a wind-tunnel. The bodies were mounted on a type K thermocouple inserted laterally between the mesothoracic and metathoracic segments. A second thermocouple, below the tunnel, measured the ambient temperature T_a. The wind-tunnel was that described in Wakeling and Ellington (1997*a*), and the thermocouples were the same as described above. The dragonfly was heated by a lamp to a thoracic temperature T_b greater than 50 °C and then allowed to cool while temperatures were recorded for a period of 5 min. When an object is warmed from the outside and then cooled, the surface will initially be warmer than the core (May, 1976). For this reason, specimens were permitted to cool by 5 °C to reverse the temperature gradient before using the data to calculate conductance. Experiments were repeated at air speeds of 0, 1 and 2 m s^{-1}, measured using an Airflow AV-2 rotating-vane anemometer. The room temperature was approximately 28 °C and in sunlight, so the radiant heat losses approximated those during the filmed flights (Wakeling and Ellington, 1997*b*).

The cooling of dead dragonflies is passive and follows the Newtonian law of cooling:

$$\frac{dT_b}{dt} = k(T_b - T_a) , \quad (36)$$

where k is the Newtonian cooling constant, given by the gradient of the linear regression of $\ln(T_b - T_a)$ against time.

The conductance C is given by the product of the cooling constant, the specific heat H of the dragonfly and its mass m:

$$C = -kHm , \quad (37)$$

where the value of the specific heat of dragonfly tissue is taken as 3.37 J kg^{-1} °C^{-1} (May, 1979).

The power for heat production by the thoracic muscles during flight, P_{heat}, is calculated from the thoracic temperatures immediately after flight and the value of conductance appropriate to the relative flight velocity:

$$P_{heat} = C(T_b - T_a) . \quad (38)$$

Muscle efficiency

Muscle efficiency is the ratio of mechanical work to the sum of heat and work. Preliminary investigations showed that P_{acc} for these flights was less than the aerodynamic power, and so the mechanical power is equal to P_{aero}. The muscle efficiency η_m is therefore:

$$\eta_m = \frac{P_{aero}}{P_{aero} + P_{heat}} . \quad (39)$$

Results

The flight sequences occurred at varying velocities and thrusts, and hence the calculated results depend simultaneously on both these variables. It must be appreciated that trends against either velocity or thrust cannot be totally isolated.

Quasi-steady lift coefficients

The quasi-steady analysis predicts that the *S. sanguineum* flights occurred at $\bar{C}_L \leqslant 1.8$, and the *C. splendens* flights at $\bar{C}_L \leqslant 1.6$ (Table 2; Fig. 3). In fact, all except one of the *S. sanguineum* flights occurred at $\bar{C}_L \leqslant 1.0$ and, in general, the

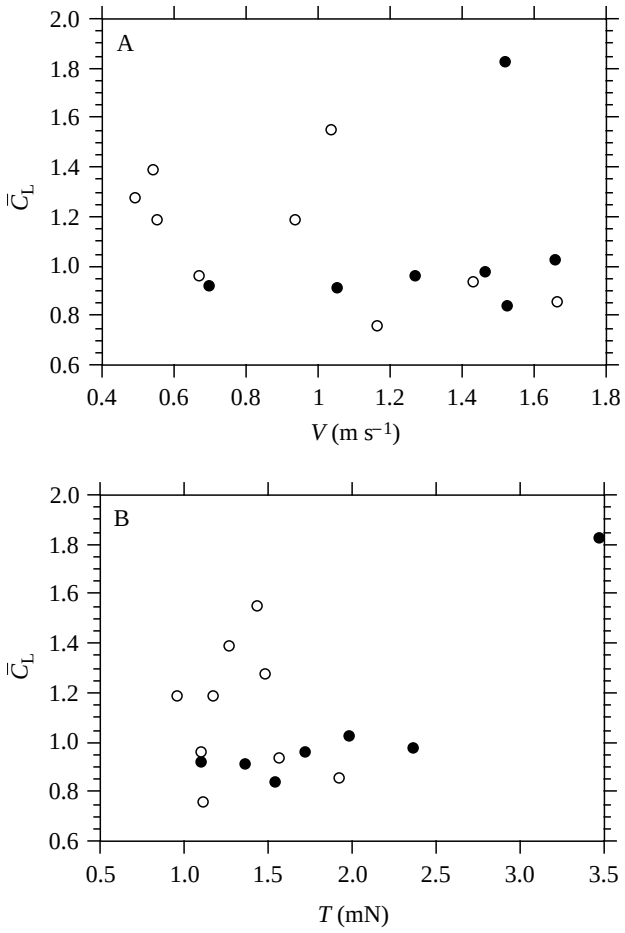

Fig. 3. Mean lift coefficients C_L plotted against velocity V (A) and thrust T (B). *Sympetrum sanguineum* and *Calopteryx splendens* are represented by filled and open circles, respectively.

dragonfly flew with lower $\bar{C}_L$ than the damselfly for any given velocity or thrust.

The *S. sanguineum* values of $\bar{C}_L \leqslant 1.0$ are within the range of C_L values which the wings can generate in a steady flow (see Wakeling and Ellington, 1997*a*), and so flights over the range $0.70<V<1.66$ could be explained by quasi-steady aerodynamics. Dragonfly lift coefficients may reach 1.8 with first-order unsteady mechanisms, i.e. unsteady separated flow and dynamic stall (Azuma *et al.* 1985), and so the extraordinarily high $\bar{C}_L$ for SSan5.1 may be explained by these mechanisms. This flight was unusual with a small value of α' (–24°, Table 2), and so there was a relatively smaller Z component of V than for the other dragonfly flights. The vertical factors A_Z and B_Z were thus small, and subsequently a larger value of $\bar{C}_L$ was required to solve the force balance of equation 25. This flight illustrates how the wings must operate at higher $\bar{C}_L$ to generate the required thrust when the angle between the velocity direction and the stroke planes is small.

The $\bar{C}_L$ values for *C. splendens* are generally greater than those for *S. sanguineum*. The main kinematic differences between the wingstrokes of these two species are the lower wingbeat frequency and greater stroke amplitude for *C. splendens*, and the fact that the damselfly performs a clap and fling at the dorsal end of its stroke (Wakeling and Ellington, 1997*b*). The wingbeat frequency and stroke amplitude both affect the flapping velocity and hence the lift of the wing. The enhancement of $\bar{C}_L$ for *C. splendens* may therefore be due to the clap-and-fling mechanism, which generates more lift for a given mean wing velocity.

The analysis assumes that both wing pairs operate at the same $\bar{C}_L$, and then calculates the thrust partitioning $\hat{T}_f$ between the fore- and hindwings. For sequences in which the fore- and hindwing kinematics differ, particularly for the damselfly where they perform different degrees of partial fling, this assumption may be inadequate. Nevertheless, it does provide a value for the minimum $\bar{C}_L$ at which all the wings must be operating and an indication of the thrust partitioning. For all *S. sanguineum* flights except one, the forewing thrust $\hat{T}_f$ was less than 0.5, and hence the hindwings provided the most aerodynamic force (Table 2). Values for *C. splendens* show $\hat{T}_f \approx 0.5$, with the fore- and hindwing pairs sharing the aerodynamic load nearly equally. The difference in thrust partitioning between *S. sanguineum* and *C. splendens* may be attributed to their wing areas. The dragonfly hindwings have a larger area than the forewings (Table 1) and so would generate more aerodynamic force for the same kinematics and $\bar{C}_L$; in contrast, the damselfly fore- and hindwings are of similar area and so would generate similar aerodynamic forces for the same kinematics and $\bar{C}_L$.

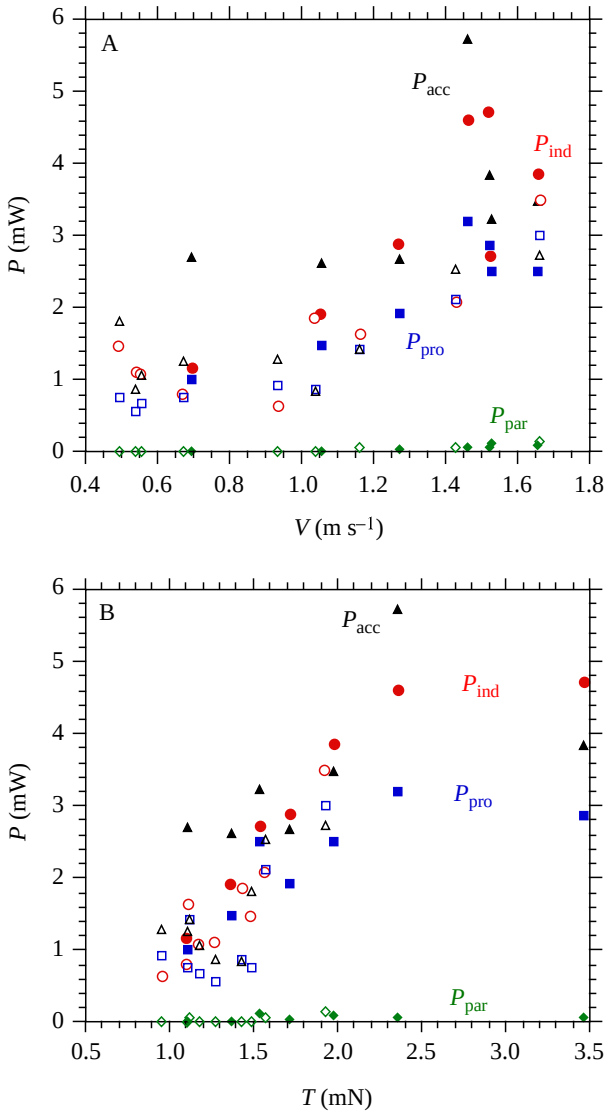

Fig. 4. Individual mechanical power components plotted against velocity V (A) and thrust T (B). *S. sanguineum* and *C. splendens* are represented by filled and open symbols, respectively. Green diamonds are for parasite power P_{par}, blue squares for profile power P_{pro}, red circles for induced power P_{ind}, and black triangles for inertial power P_{acc}. The values for P_{ind} implicitly include P_{par}.

Induced power

Induced power is similar for both *S. sanguineum* and *C. splendens* and shows a general increase with both velocity and thrust (Table 3; Fig. 4); there is a stronger relationship for the increase with thrust. For horizontal flights at nearly constant thrusts equal to body weight, Pennycuick (1975) predicts that $P_{ind} \propto 1/V$ and hence decreases with increasing velocity. The reason for the observed increase of P_{ind} with V can be attributed to the correlation between thrust and velocity for these flights (Wakeling and Ellington, 1997*b*). P_{ind} is more strongly dependent on T than on V, and hence the relationship with V is partially obscured by the effect of T.

Profile power

Profile power is also similar for both species of dragonfly (Table 3) and shows an increase with both V and T (Fig. 4). The increase with V is expected because, at higher velocities, the relative velocity and thus D_{pro} increase. The increase with T is because additional aerodynamic force is generated by the wings beating at larger stroke amplitudes for the dragonfly

Table 3. *Components of mechanical power during flight*

Flight	m (mg)	$\hat{m}_m$	P_{ind} (mW)	P_{pro} (mW)	P_{acc} (mW)	P_{aero} (mW)	P^*_{aero} (W kg^{-1})
SSan2.1	121.9	0.492	3.85	2.52	3.49	6.92	115.3
SSan2.3	121.9	0.492	1.92	1.49	2.61	3.65	60.9
SSan5.1	133.0	0.483	4.70	2.86	3.83	7.84	122.1
SSan5.2	133.0	0.483	1.16	1.00	2.71	2.27	35.4
SSan6.1	111.5	0.479	4.60	3.20	5.73	8.36	156.2
SSan6.2	111.5	0.479	2.71	2.50	3.24	5.58	104.3
SSan9.1	139.3	0.489	2.88	1.94	2.68	5.20	76.3
CS1.1	91.0	0.327	0.79	0.76	1.26	1.61	54.3
CS1.3	91.0	0.327	1.10	0.56	0.87	1.73	58.2
CS2.2	93.6	0.367	1.87	0.88	0.84	2.94	85.6
CS2.3	93.6	0.367	1.64	1.43	1.42	3.34	97.3
CS2.5	93.6	0.367	1.09	0.69	1.06	1.88	54.6
CS3.2	123.6	0.342	2.09	2.13	2.54	4.50	106.4
CS3.3	123.6	0.342	0.63	0.93	1.28	1.63	38.4
CS3.5	123.6	0.342	3.50	3.02	2.74	7.02	166.1
CS4.2	119.1	0.353	1.46	0.77	1.82	2.34	55.8

m, mass; $\hat{m}_m$, non-dimensional muscle mass; P_{ind}, induced power; P_{pro}, profile power; P_{acc}, inertial power; P_{aero}, aerodynamic power; P^*_{aero}, muscle mass-specific aerodynamic power.

SSan, *Sympetrum sanguineum*; CS, *Calopteryx splendens*.

and at higher frequencies for the damselfly (Wakeling and Ellington, 1997*b*), both of which increase the relative velocity.

Inertial power

P_{acc} shows a general increase with both V and T (Fig. 4), again an expected result because at higher V and T the wings must beat at higher velocities to generate the required forces, and this entails higher P_{acc} costs. The inertial power costs for *S. sanguineum* are typically double those for *C. splendens*. The dragonfly wings have lower moments of inertia than those of the damselfly because their mass and area are distributed closer to the wing bases; however, their higher wingbeat frequencies and maximum wing velocities lead to the higher values for P_{acc}. For all except one of the flights of both species, P_{acc} is less than P_{aero} (Table 3).

Aerodynamic power

Graphs for aerodynamic power P_{aero} as functions of V and T are shown in Fig. 5, and for muscle mass-specific P^*_{aero} in Fig. 6. P_{aero} is generally lower for *C. splendens* than for *S. sanguineum* at any given V; this again can be attributed to the clap-and-fling mechanism, which is the major kinematic difference between the two, as being a more efficient way of generating aerodynamic force. The damselfly has a lower proportion of muscle mass $\hat{m}_m$ than the dragonfly (Table 3) so, despite the fact that both species were of similar mass, the muscle mass-specific P^*_{aero} is greater for *C. splendens* than for *S. sanguineum*.

S. sanguineum shows a monotonic increase in P_{aero} with speed, but it slightly increases for *C. splendens* at low speeds.

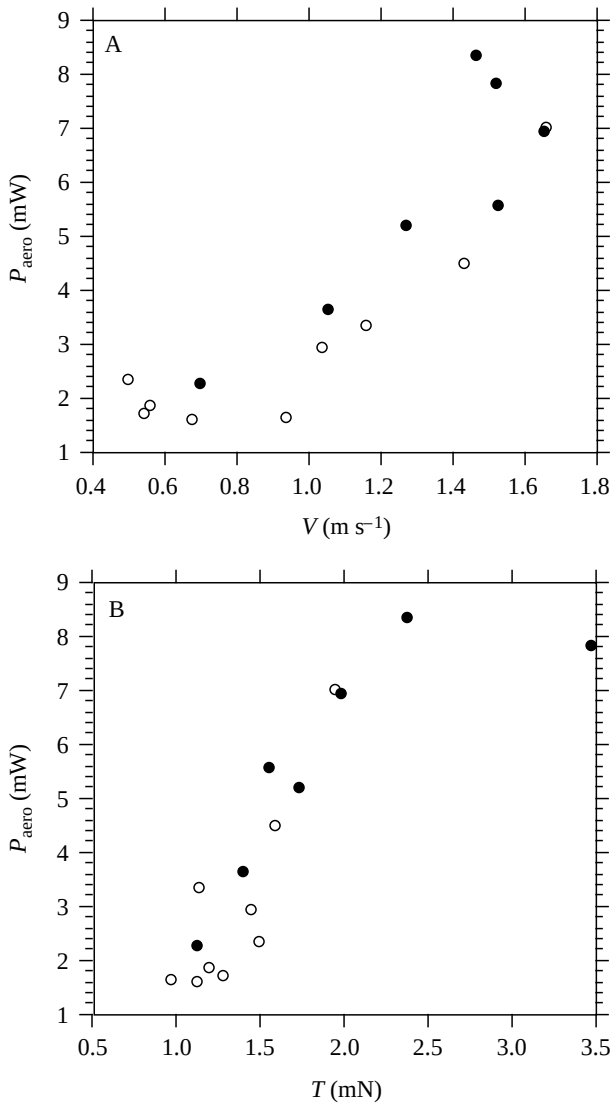

Fig. 5. Aerodynamic power P_{aero} plotted against velocity V (A) and thrust T (B). *S. sanguineum* and *C. splendens* are represented by filled and open circles, respectively.

The damselfly flights extend to lower values of V and advance ratio J than those of the dragonfly, so the reason for the dragonfly not showing an increase in P_{aero} at the lower velocities may be the more restricted speed range. Again, the true shape of the relationship between P_{aero} and V may be obscured by correlations with T.

Both species showed an increase in P_{aero} with T; this is to be expected as high thrusts necessarily require high P_{ind}.

The maximum P^*_{aero} values were 156 W kg^{-1} and 166 W kg^{-1} for *S. sanguineum* and *C. splendens*, respectively. Because P_{acc} is smaller than P_{aero}, these are also the maximum mechanical power outputs from the muscle and are unaffected by the extent of elastic storage.

Heat production

Values for the Newtonian cooling constant k are shown in

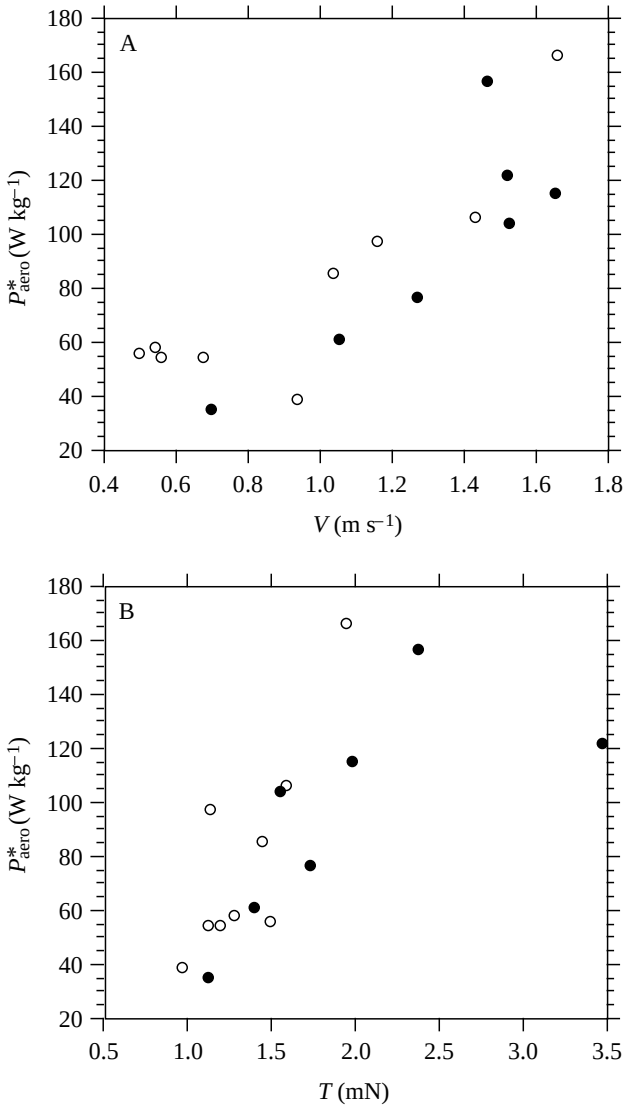

Fig. 6. Muscle mass-specific aerodynamic power P^*_{aero} plotted against velocity V (A) and thrust T (B). *S. sanguineum* and *C. splendens* are represented by filled and open circles, respectively.

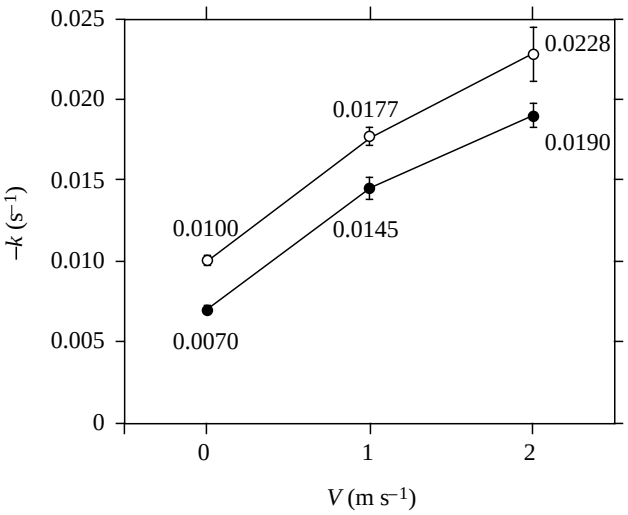

Fig. 7. Newtonian cooling constant k as a function of air velocity V during passive cooling in a wind-tunnel. Data for *S. sanguineum* are given by filled circles and data for *C. splendens* by open circles. Mean values for $-k$ (N=4) are given, and error bars indicate the standard error of the means (S.E.M.).

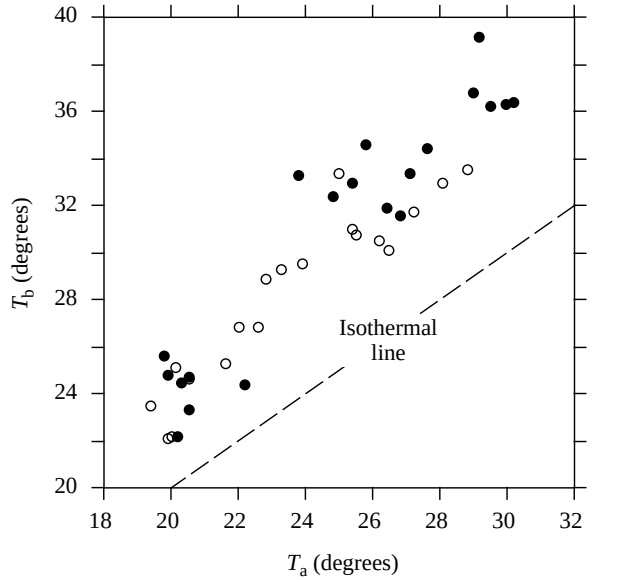

Fig. 8. Thoracic temperatures T_b immediately after flight plotted against ambient temperature T_a during each flight. Data for *S. sanguineum* are given by filled circles and data for *C. splendens* by open circles.

Fig. 7. As a result of convective cooling, k almost doubles when the airspeed increases from 0 to 1 m s^{-1}, and then shows a lesser increase as speed increases to 2 m s^{-1}. The relative flight velocities V_r were $1.13<V_r<2.05$ m s^{-1} and $0.92<V_r<1.91$ m s^{-1} for *S. sanguineum* and *C. splendens*, and so values of k during flight are well represented by the respective means of k=–0.017 s^{-1} and k=–0.020 s^{-1} from cooling in an air flow of 1–2 m s^{-1}.

Thoracic temperatures immediately after flight are shown in Fig. 8. The mean values for muscle mass-specific heat production were 663 W kg^{-1} and 838 W kg^{-1} for *S. sanguineum* and *C. splendens*, respectively.

Discussion

Current understanding of dragonfly aerodynamics is still limited by our poor knowledge of the nature of the flow interactions between the fore- and hindwings. Dragonflies can beat all their wings independently, and they can alter the phase relationships between the fore- and hindwings; near synchronous wingbeats may be used to generate more aerodynamic force than the usual dragonfly mode of ‘counterstroking’ (Alexander, 1984, 1986; Rüppell, 1989). Mechanical models have shown that changing the phase relationship between the fore- and hindwings can, indeed, alter

the force production (Luttges, 1989), and similar conclusions have been predicted from theory (Lan, 1979; Azuma *et al.* 1985). Vortices shed from the wings interact, and the resultant force cannot be predicted from the kinematics of the individual wings alone (Saharon and Luttges, 1988). Until the nature of the wing interactions is better understood, the effects of kinematic variations for individual wings cannot be predicted with confidence.

The approach taken in the present analysis uses a single actuator disc for all four wings in the induced power calculations and investigates the net mass flux of air into the far wake. Problems created by flow interactions between the wings are thus circumvented. A more detailed aerodynamic description of dragonfly flight will only be possible when the precise flows around each wing can be accurately modelled. Nonetheless, the results from the present study are useful for assessing dragonfly flight performance and for comparisons with other insects. Additionally, the methods used here for considering the effects of accelerations are applicable to insects with one functional pair of wings.

Quasi-steady lift coefficients

The quasi-steady $\bar{C}_L$ for *S. sanguineum* appears surprisingly low from the present study. For all except one of its flights, $0.8<\bar{C}_L<1.0$, despite the fact that the advance ratio was consistently low ($J<0.5$, Wakeling and Ellington, 1997*b*) and so the flights were approaching hovering. Previous authors who found high $\bar{C}_L$ values for the dragonfly (Osborne, 1951; Weis-Fogh, 1967; Norberg, 1975) all studied flights in which the stroke planes were steeply inclined, i.e. where they were not nearly normal to the thrust. The flight SSan6.1 had a reasonably inclined stroke plane with $\beta'=-18°$, but all the other *S. sanguineum* flights were in the range $-12°<\beta'<8°$ and thus were nearly normal to the thrust. *S. sanguineum* can generate unsteady lift from its wings: flight SSan5.1 required $\bar{C}_L$ equal to 1.8, a value which is incompatible with quasi-steady assumptions, and in the field *S. sanguineum* hovers with a horizontal body and inclined stroke planes. However, it tends to 'hover' facing into the wind whenever there is any breeze, and this effectively gives it a forward velocity. For accelerated flight, as in the present study, dragonflies may adopt kinematics with stroke planes nearly normal to the thrust more often than has previously been thought. The upstroke is thus recruited for an equal share of the thrust production, halving $\bar{C}_L$ compared with a strongly inclined stroke that relies on the downstroke alone for thrust.

The quasi-steady $\bar{C}_L$ for *C. splendens* is generally higher than for *S. sanguineum*: $0.8<\bar{C}_L<1.6$. The mean wing velocity is lower for the damselfly, mainly because its wingbeat frequency is half that of the dragonfly. However, the body mass and wing area are similar for the two species. For a given level of thrust generation, the damselfly must operate its wings at higher $\bar{C}_L$, and this is indeed what happens. The extra lift for the damselfly wing may be derived from the clap-and-fling mechanism, and has already been discussed in Wakeling and Ellington (1997*b*).

The values for $\bar{C}_L$ have been calculated on the assumption that useful lift is produced on both the up- and downstrokes. For damselfly flights where there is a strong clap and fling, this assumption may not be adequate. As the wings are flung apart, a flow of air into the opening gap creates a circulation about each wing; these circulations are created prior to, and completely independently of, the translatory motion of the wings. Downstroke circulation is thus enhanced by circulation generated at the preceding fling. At the start of the upstroke, however, the isolated wings must fight the Wagner effect which could be exacerbated by the shed vorticity from the downstroke. Upstroke circulation may thus be lower than from quasi-steady predictions. In the extreme case, all the lift may be generated during the downstroke, with none being generated during the upstroke. $\bar{C}_L$ can be calculated for such cases by taking a value of zero for $I_{L,Z(u)}$ in equation 22: profile drag still occurs during each half-stroke, but lift is only produced on the downstroke. Such estimates of $\bar{C}_L$ based on lift from the downstroke alone represent the upper limits of $\bar{C}_L$ and are given in Table 4. It should be noted that, while there may be some justification for these values for some of the damselfly flights, the original assumption of both upstroke and downstroke lift is probably more appropriate to the dragonfly and the rest of the damselfly flights.

The damselfly utilises its highest $\bar{C}_L$ during its lowest-velocity flights. This may underlie differences in its flight behaviour when compared with the dragonflies. Field observations show that dragonflies typically fly quickly through the large airspaces above a body of water whilst damselflies fly more slowly, manoeuvring around the

Table 4. *Mean lift coefficient and thrust partitioning assuming that* $C_{D,pro}=0.2$ *and that lift is generated purely on the downstroke*

Flight	$\hat{T}_f$	$\bar{C}_L$
SSan2.1	0.483	1.79
SSan2.3	0.569	1.71
SSan5.1	0.345	3.15
SSan5.2	0.320	1.91
SSan6.1	0.440	2.34
SSan6.2	0.409	1.71
SSan9.1	0.487	2.00
CS1.1	0.566	2.25
CS1.3	0.537	2.68
CS2.2	0.490	2.59
CS2.3	0.645	1.67
CS2.5	0.538	2.36
CS3.2	0.514	1.49
CS3.3	0.558	2.08
CS3.5	0.440	1.82
CS4.2	0.426	2.88

$\bar{C}_L$, mean lift coefficient; $\hat{T}_f$, non-dimensional forewing thrust; $C_{D,pro}$, profile drag coefficient.

SSan, *Sympetrum sanguineum*; CS, *Calopteryx splendens*.

vegetation at the water's edge. The clap-and-fling mechanism may be useful during the slow precision flight of damselflies. Dragonflies, in contrast, have become adapted to faster flights in more open airspaces and have done so with modifications to their wing shapes (Wakeling, 1997) and thoracic structures that include a reduction of the stroke amplitude available to the forewings (Pfau, 1986, 1991). These modifications make the dragonfly less suited to performing flings, but flings may not be necessary during higher-velocity flights. Nonetheless, dragonflies are adept at hovering (Norberg, 1975), and they may achieve this by exploiting circulation generated during isolated wing rotations.

Inefficiencies in the momentum jet

The 'vertical' component of the profile drag results in an effective increase in thrust and induced power of 12 %, on average, for the momentum jet. This additional thrust required to overcome the profile drag can be considered an inefficiency in the wake. This effect may be accommodated by a correction factor k_{ind} to the Rankine–Froude estimate for induced power that is greater than 1.2. The precise value of k_{ind} may depend on the ratio of the profile to the induced drag, and so may be different for dragonflies than for insects with one functional pair of wings. Justification for such a modification to k_{ind} will have to await confirmation from studies on other insects.

Local circulation method

Azuma *et al.* (1985), Azuma and Watanabe (1988) and Azuma (1992) state that dragonfly flight can be explained using quasi-steady assumptions alone. They used a modified local circulation method from helicopter analysis to analyse dragonfly flight and obtained no unusually high lift coefficients. This is in contrast to the conclusions from all other studies on dragonfly flight. Their methods were originally developed for helicopter flight where the rotors beat in a nearly horizontal plane, with the thrust perpendicular to this plane and thus nearly vertical. In adapting their first 'simple analysis' to dragonfly flight, Azuma *et al.* (1985) maintained the assumption that the thrust is perpendicular to the stroke plane, even though the flights involved inclined stroke planes. If the major force acting on the dragonfly is its weight, which is vertical, then the net aerodynamic force must also be vertical and is generated by a horizontal actuator disc. The stroke planes for their dragonflies were not horizontal, however, and their actuator disc lies in the stroke plane rather than in the horizontal; this is where their simple analysis departs from the methods used here and leads to erroneous conclusions.

Azuma *et al.* (1985) filmed *Sympetrum frequens* during steady, slow climbing flight, i.e. without acceleration. The low parasite drag was neglected, which is a reasonable assumption, so the only net force is the vertical weight support. However, the thrust is calculated normal to the stroke planes with a vertical component to match $m\boldsymbol{g}$; as the stroke planes are inclined to the horizontal, there would be a corresponding horizontal force component of $0.81m\boldsymbol{g}$. The induced velocity was calculated using a form of equation 8, i.e. for a flight velocity normal to the actuator disc; V was indeed normal to the disc, but this equation gives an induced velocity also normal to the disc. Because the only net force on the dragonfly is the vertical $m\boldsymbol{g}$, the induced velocity should be vertical instead. Using equation 6 with their data yields an induced velocity over six times their value and greater than V_X.

They calculate the net forces over the wingstroke using a modified blade-element analysis. With V and w being normal to the stroke planes, the relative velocity V_r is also normal to the stroke planes. It is implicitly assumed that the upstroke and downstroke contribute equally to thrust generation. Because w should be vertical, however, V_r should not be normal to the stroke planes. The wings actually beat with an asymmetry between the up- and downstrokes because they are inclined to the relative velocity, and in such cases $\bar{C}_L$ must be higher to support the required thrust. An attenuation coefficient C_{hf} equal to 0.3 was used to model the effect of the forewing's induced velocity on the hindwings; i.e. 30 % of that induced velocity acted on the hindwing. This value seems very low and should probably be closer to 2 (Stepniewski and Keys, 1984). Finally, they solve simultaneously the conditions that the net horizontal force is zero and that the vertical force balances the weight. However, as stated above, this analysis implicitly creates a large horizontal force which is subsequently ignored. Additionally, instantaneous lift forces were calculated from a $C_L(\alpha)$ function with $C_{L,max}$=1.8; this clearly does not describe a dragonfly wing under steady-state conditions (Wakeling and Ellington, 1997*a*).

Using the methods presented in the present study, their data for the *S. frequens* flight result in $\hat{T}_f$=0.46, $\bar{C}_L$=3.9 and P^*_{aero}= 52 W kg^{-1}. This slow flight involves a mean lift coefficient that certainly cannot be explained by quasi-steady assumptions, in contradiction to their conclusion.

A local circulation method was then presented by these authors for analysing the flight of *S. frequens* (Azuma *et al.* 1985) and *Anax parthenope* (Azuma and Watanabe, 1988). To overcome their main objection to the 'simple analysis' (that the induced velocity was constant across the actuator disc in both time and space), a time-varying induced velocity is introduced; the analysis is computationally more complex and only a skeleton of the methods is presented in the two papers. Nonetheless, the results and conclusions from the two methods are similar. The time-varying induced velocity in the local circulation method gives mean horizontal and vertical forces that are small and balance weight support, respectively. However, without further information on how the initial kinematic and force data were incorporated into the local circulation method, its suitability for the analysed dragonfly flight cannot be assessed.

Both methods discussed above require that each wing pair supports nearly half the thrust; this was an imposed restriction on the simple analysis, but it emerged as a solution in the local circulation method (certainly for *Anax parthenope* case 4, for which graphical data are presented). For both methods, the interference from the hindwing on the forewing was considered negligible and was ignored. Thus, calculations for the

forewings supporting half the thrust will be irrespective of any wing interactions and can be treated as an insect beating one pair of wings. The methods of the present study predict that the forewings alone of *Anax parthenope* would have operated at $1.9<\bar{C}_L<6.9$ if they supported half the thrust, and thus quasi-steady lift generation is unable to account for the aerodynamics of these flights.

Muscle power output

For all except one of the flights in the present study, inertial power was lower than aerodynamic power. The mechanical power output of the flight muscles is thus equal to the aerodynamic power regardless of the degree of elastic storage (Dickinson and Lighton, 1995). Elastic elements within the flight motor system are certainly able to store and return most of the inertial energy. Various elastic systems have been found in the thoraces of insects (Alexander, 1988); indeed, Weis-Fogh (1960) found an elastic tendon in dragonflies, including *Sympetrum* and *Calopteryx* species, which was a cylinder of pure resilin interpolated in the apodemes of some wing muscles. Elastic torque measurements for *Aeshna grandis* show that approximately 75 % of the inertial energy can be stored and released by both the wing ligaments and the muscle fibres themselves (Weis-Fogh, 1972). Non-fibrillar muscle fibres can store up to $2.5\,J\,kg^{-1}$ of elastic energy (Alexander and Bennet-Clark, 1977), and this would correspond to 50 and $100\,W\,kg^{-1}$ at the respective wingbeat frequencies of *S. sanguineum* and *C. splendens*, making up 93 % and 78 %, respectively, of the maximum inertial power. Even if elastic elements in the thorax returned none of the inertial power, the inertial power expended at the beginning of each half-stroke would be recovered as the wing decelerates during the second half-stroke, contributing to the aerodynamic power costs at the end of each half-stroke. The net mechanical power output from the muscles thus equals the aerodynamic power, regardless of elasticity assumptions, and is 156 and $166\,W\,kg^{-1}$ for *S. sanguineum* and *C. splendens*, respectively. It should be noted that during a complete clap and fling, in which the left and right wings come to a halt as they touch, much of the kinetic energy might be lost as heat and sound from the wings and could not be stored in thoracic elements. However, the damselfly flights typically involve partial flings in which the wings do not halt at the top, and so there is still scope for elastic storage.

These maximum muscle power outputs of around $160\,W\,kg^{-1}$ are at the upper end of power outputs, both measured and modelled, for insect synchronous flight muscle. Weis-Fogh and Alexander (1977) proposed that for non-fibrillar and vertebrate striated muscle the maximum power output is governed by the intrinsic contraction frequency of the muscle; with a high intrinsic contraction frequency of $25\,s^{-1}$ and contraction over 15 % of its resting length, the maximum power is approximately $250\,W\,kg^{-1}$. Pennycuick and Rezende (1984) simplified this model and argued that power was the product of the frequency imposed by the biomechanics and the work done per unit muscle mass. The simplified model suggests that maximum power would asymptotically approach a limit of $860\,W\,kg^{-1}$ as contraction frequency increases, but estimates powers of $400\,W\,kg^{-1}$ for synchronous muscle at the wingbeat frequencies typical of Odonata. Ellington (1985) further modified this model to account for the volume of sarcoplasmic reticulum and, assuming that locust muscle contracted by 5 % of its length at the measured intrinsic contraction frequency of $9\,s^{-1}$, calculated a revised value of $80\,W\,kg^{-1}$ for this classic synchronous flight muscle.

Josephson (1985) studied the power output of tettigoniid synchronous flight muscle using a work loop method first developed by Machin and Pringle (1959) for asynchronous muscle. By measuring muscle tension while an oscillating length change is imposed on it, *in vitro* results should more closely approximate *in vivo* performance. Maximum power outputs for this and similar studies have recorded $76\,W\,kg^{-1}$ for tettigoniid flight muscle (Josephson, 1985), $33\,W\,kg^{-1}$ for locust flight muscle (Mizisin and Josephson, 1987) and $90\,W\,kg^{-1}$ for hawkmoth flight muscle (Stevenson and Josephson, 1990). In their study of hawkmoth muscle, Stevenson and Josephson (1990) found that maximum power output increased with temperature, and they recorded maxima of $130\,W\,kg^{-1}$ for two preparations at 40 °C. They also showed that the values from other studies were comparable with the hawkmoth results when temperature was taken into account. Their value of $130\,W\,kg^{-1}$ is the highest measured from an insect synchronous flight muscle. Willmott (1995) has recently estimated a value of $150\,W\,kg^{-1}$ for hawkmoth flight muscle using aerodynamic arguments.

Marden (1987) has estimated the maximum forces produced by insects during take-off by attaching weights to them. Ellington (1991) reanalysed his data, correcting the induced power calculations and adding a further 30 % as a rough estimate for the profile power. The present study has shown that profile power for two pairs of wings is typically 75 % of the induced power, and so the maximum aerodynamic power recalculated from Marden's data would be $150\,W\,kg^{-1}$ for Odonata.

Aerodynamic costs of flight

For flight at constant velocities, the aerodynamic power changes with velocity. There is some debate about whether the power curves are U-shaped or J-shaped (see Ellington, 1991). Whatever the precise shape, however, the curves share several common features: P^*_{aero} is smallest at some intermediate speed, often with a very broad minimum, and increases rapidly at higher velocities, reaching the maximum mechanical power output at the maximum velocity possible for the animal. Finding this maximum velocity is experimentally difficult, because animals are reluctant to cooperate at such high performance levels. Hence, this velocity is commonly estimated by extrapolation of P^*_{aero} to the maximum power output expected from the muscle.

The P^*_{aero} curves from the present study show P^*_{aero} to be less than $60\,W\,kg^{-1}$ for $0.5<V<1.0\,m\,s^{-1}$ and then to increase at higher velocities for both *S. sanguineum* and *C. splendens*. The maximum velocities of $1.7\,m\,s^{-1}$ occur at power outputs which

are likely to be near the maximum possible for odonatan flight muscle. These maximum velocities, however, do not represent the maximum velocities possible for these species. The P^*_{aero} costs increase with both velocity and thrust, and the flights at the highest V also occur at some of the highest values of T. Were these flights to have been horizontal at a constant velocity, then P^*_{aero} would probably have been smaller. During one of the gliding sequences from Wakeling and Ellington (1997*a*), a velocity of 2.6 m s^{-1} was recorded for *S. sanguineum*, showing that they can indeed fly at velocities greater than 1.7 m s^{-1} if they are not simultaneously accelerating.

P^*_{aero} increases with thrust for both *S. sanguineum* and *C. splendens*. It is important for both of these species to generate thrusts of at least $\hat{T}\approx2.3$ so that males can support heavier females while flying in tandem during mating (relative masses from Grabow and Rüppell, 1995). The maximum $\hat{T}$ values recorded in the present studies were 2.65 and 1.59 for *S. sanguineum* and *C. splendens*, respectively. More data points are desirable at the higher thrusts, but the data reported here suggest that *S. sanguineum* can comfortably achieve mating flight, whereas *C. splendens* will be struggling to achieve $\hat{T}=2$ for much less than 160 W kg^{-1} muscle power output.

Heat production

Cooling constants have been measured for a number of dragonfly species by May (1976); the interpolated value for a temperate species with a 68 mg thorax (typical of *S. sanguineum*) is k=–0.0056 in still air, with the spread of the data covering the value of k=–0.0070 reported here. The thorax of *C. splendens* is smaller than that of *S. sanguineum* and, because of the scaling of conductance, the larger value found for k (–0.0100) for *C. splendens* is to be expected. The rate of heat loss increases in an air flow (Church, 1960*b*; May, 1976; Casey, 1976, 1980, 1981), and this can lead to two- or threefold increases in the cooling constant for the speeds at which these flight sequences occurred (Fig. 7). Heat loss due to evaporative cooling is low in small flying insects (Church, 1960*a*); *Sympetrum* species have 85 % of their thoracic wall insulated by air sacs (Church, 1960*b*); and percher species in general have little physiologically facilitated heat transfer between the thorax and abdomen (Heinrich and Casey, 1978; Heinrich, 1993). Heat production estimates based on conductance values from dead dragonflies should thus be fairly reliable. Indeed, the mean cooling constants for live dragonflies cooling to 30 °C differ by no more than 3 % from those for dead dragonflies (May, 1976).

The mean muscle mass-specific heat production during the flights recorded in the present study are 663 and 838 W kg^{-1} for *S. sanguineum* and *C. splendens*, respectively. The mean muscle mass-specific metabolic power is the sum of these mean heat productions and the mean aerodynamic powers (Table 3) and is 759 and 918 W kg^{-1} for *S. sanguineum* and *C. splendens*, respectively. May (1995) presents metabolic rates during flight for Anisoptera in the body mass range 170–3160 mg; the data include his own estimates from heat production and Polcyn's (1988) respirometry measurements. The data show considerable scatter, but there is a general increase in mass-specific metabolic rate with decreasing body size. *S. sanguineum* falls below the range of May's data, but its rate falls within the 95 % confidence limits for the extrapolated trend. The metabolic rates also compare favourably with those measured for moths: Casey (1981) found thoracic mass-specific metabolic rates during hovering of 551 W kg^{-1} and 1591 W kg^{-1} for two moth species of body mass 90–100 mg.

Resting metabolic rates of a 120 mg dragonfly may typically be 11 W kg^{-1} muscle mass (May, 1979). Compared with the estimated metabolic rates of *S. sanguineum* and *C. splendens*, this would give a metabolic scope of 70–80, which lies comfortably within the range of 50–100 typically found for flying insects (Ellington, 1984*d*).

Muscle efficiency during flight

Muscle efficiencies scale with animal size for locomotory activities. With increasing size, the mass-specific metabolic rate of animals decreases, but the mass-specific cost of transport is reasonably independent of size; hence, larger animals perform the same mass-specific work for a lower metabolic cost and are thus more efficient. Muscle efficiencies in vertebrate locomotion decrease from 70 % for humans and kangaroos to 7 % for a 30 g quail (Heglund and Cavana, 1985); the high values are largely due to substantial elastic energy return from the muscle–tendon complex. The highest recorded muscle efficiency from an isolated vertebrate muscle is 37 % (DeHaan *et al.* 1989). Decreasing muscle efficiency with size has been shown for a variety of moth species (Casey, 1989). For a range of euglossine bees, efficiency decreased from 16 % to a mere 4 % over a corresponding mass decrease from 1000 to 80 mg (Casey and Ellington, 1989), assuming perfect elastic return of inertial power. The muscle efficiency during hovering (also assuming perfect elastic storage) has been estimated at 6 % for *Bombus*, 5 % for *Apis* and 8 % for *Eristalis* (Ellington, 1984*d*), and at 11 % for *Drosophila* flight regardless of elastic storage mechanisms (Dickinson and Lighton, 1995). Muscle efficiencies during insect flight are typically much lower than those found for vertebrate muscle, but this can be attributed to their small size. The values depend on the assumed extent of elastic storage; with no elastic return, the mechanical power output is greater, and so the efficiency is higher. However, it is currently thought that substantial elastic storage occurs during insect flight. In order to resolve this dilemma, Josephson and Stevenson (1991) measured the O_2 consumption and the power output simultaneously during cyclic work loop experiments on locust flight muscle. This direct measurement of muscle efficiency gave a value of 6 %, confirming that insect flight muscle does indeed operate at very low efficiencies.

The mechanical power outputs from the present study, and thus also the muscle efficiencies, are unaffected by assumptions of elastic storage because the inertial power is less than the aerodynamic power. The mean muscle efficiencies are 12.6 % and 8.7 % for *S. sanguineum* and *C. splendens*, respectively. These efficiencies are both reasonable given the

other values for insects, and they are at the upper limit of what can be expected from insect flight muscle.

Dragonfly ancestors, the Protodonata, are amongst the earliest winged insect fossils, and the dragonfly mode of flight has persisted for 300 million years (Wootton, 1974; May, 1982). The evolution of the more modern, neopteran, insects has superseded the odonates, and their modern mode of flight with one functional pair of wings can be considered to be evolutionarily more advanced. Dragonflies are still a major aerial insect predator, however, and they have by no means been ousted by their younger relatives. Indeed, modern dragonflies can out-manoeuvre and prey upon neopteran insects. The dragonflies' success can be attributed to the exceptional aerodynamic properties of their wings, their powerful and efficient flight muscles, and one of the highest ratios of flight muscle to body mass for any animal (Marden, 1989). The two sub-orders, Anisoptera and Zygoptera, have become adapted to different styles of flight: dragonflies fly rapidly in large airspaces, whereas damselflies manoeuvre through vegetation at lower speeds. These differences can be explained in terms of their different wing shapes (Wakeling, 1997), thoracic structure and the degrees of freedom available to the wings (Pfau, 1986), wingbeat kinematics (Wakeling and Ellington, 1997*b*) and their aerodynamics, with the damselfly utilising the clap-and-fling mechanism which is useful for its low speed flight.

We thank A. P. Willmott for stimulating discussions, an anonymous referee for helpful comments on the manuscripts and the BBSRC for financial support.

References

ALEXANDER, D. E. (1984). Unusual phase relationships between the forewings and hindwings in flying dragonflies. *J. exp. Biol.* **109**, 379–383.

ALEXANDER, D. E. (1986). Wind tunnel studies of turns by flying dragonflies. *J. exp. Biol.* **122**, 81–98.

ALEXANDER, R. MCN. (1988). *Elastic Mechanisms in Animal Movement*. Cambridge: Cambridge University Press.

ALEXANDER, R. MCN. AND BENNET-CLARK, H. C. (1977). Storage of elastic strain energy in muscle and other tissues. *Nature* **265**, 114–117.

AZUMA, A. (1992). *The Biokinetics of Flying and Swimming*. pp. 138–148. Berlin: Springer-Verlag.

AZUMA, A., AZUMA, S., WATANABE, I. AND FURUTA, T. (1985). Flight mechanics of a dragonfly. *J. exp. Biol.* **116**, 79–107.

AZUMA, A. AND WATANABE, T. (1988). Flight performance of a dragonfly. *J. exp. Biol.* **137**, 221–252.

BETTS, C. R. AND WOOTTON, R. J. (1988). Wing shape and flight behaviour in butterflies (Lepidoptera: Papilionoidea and Hesperioidea): a preliminary analysis. *J. exp. Biol.* **138**, 271–288.

CASEY, T. M. (1976). Flight energetics in sphinx moths: heat production and heat loss in *Hyles lineata* during free flight. *J. exp. Biol.* **64**, 545–560.

CASEY, T. M. (1980). Flight energetics and heat exchange of gypsy moths in relation to air temperature. *J. exp. Biol.* **88**, 133–145.

CASEY, T. M. (1981). A comparison of mechanical and energetic estimates of flight cost for hovering sphinx moths. *J. exp. Biol.* **91**, 117–129.

CASEY, T. M. (1989). Oxygen consumption during flight. In *Insect Flight* (ed. G. Goldsworthy and C. H. Wheeler), pp. 257–272. CRC Press, Boca Raton, Florida.

CASEY, T. M. AND ELLINGTON, C. P. (1989). Energetics of insect flight. In *Energy Transformations in Cells and Organisms* (ed. W. Wieser and E. Gnaiger), pp. 200–210. Stuttgart: Georg Thieme Verlag.

CHURCH, N. S. (1960*a*). Heat loss and body temperatures of flying insects. I. Heat loss by evaporation of water from the body. *J. exp. Biol.* **37**, 171–185.

CHURCH, N. S. (1960*b*). Heat loss and the body temperature of flying insects. II. Heat conduction within the body and its loss by radiation and convection. *J. exp. Biol.* **37**, 186–212.

COOPER, A. J. (1993). Limitations on bumblebee flight performance. PhD thesis. Cambridge University.

CORBET, P. S. (1983). *A Biology of Dragonflies* (ed. E. W. Classey). Oxon: Farrington.

DEHAAN, A., VAN INGEN SCHENAU, G. J., ETTEMA, G. J., HUIJING, P. A. AND LODDER, M. A. N. (1989). Efficiency of rat medial gastrocnemius muscle in contractions with and without an active prestretch. *J. exp. Biol.* **141**, 327–341.

DICKINSON, M. H. AND LIGHTON, J. R. B. (1995). Muscle efficiency and elastic storage in the flight motor of *Drosophila*. *Science* **268**, 87–90.

DUDLEY, R. AND DEVRIES, P. J. (1990). Flight physiology of migrating *Urania fulgens* (Uraniidae) moths: kinematics and aerodynamics of natural free flight. *J. comp. Physiol.* A **167**, 145–154.

DUDLEY, R. AND ELLINGTON, C. P. (1990). Mechanics of forward flight in bumblebees. II. Quasi-steady lift and power requirements. *J. exp. Biol.* **148**, 53–88.

ELLINGTON, C. P. (1980). Vortices and hovering flight. In *Instationäre Effekte an Schwingenden Tierflügeln* (ed. W. Nachtigall), pp. 64–101. Wiesbaden: Franz Steiner.

ELLINGTON, C. P. (1984*a*). The aerodynamics of hovering insect flight. II. Morphological parameters. *Phil. Trans. R. Soc. Lond. B* **305**, 17–40.

ELLINGTON, C. P. (1984*b*). The aerodynamics of hovering insect flight. III. Kinematics. *Phil. Trans. R. Soc. Lond. B* **305**, 41–78.

ELLINGTON, C. P. (1984*c*). The aerodynamics of hovering insect flight. V. A vortex theory. *Phil. Trans. R. Soc. Lond. B* **305**, 115–144.

ELLINGTON, C. P. (1984*d*). The aerodynamics of hovering insect flight. VI. Lift and power requirements. *Phil. Trans. R. Soc. Lond. B* **305**, 145–181.

ELLINGTON, C. P. (1985). Power and efficiency of insect flight muscle. *J. exp. Biol.* **115**, 293–304.

ELLINGTON, C. P. (1991). Limitations on animal flight performance. *J. exp. Biol.* **160**, 71–91.

ENNOS, A. R. (1989). The kinematics and aerodynamics of the free flight of some Diptera. *J. exp. Biol.* **142**, 49–85.

GRABOW, K. AND RÜPPELL, G. (1995). Wing loading in relation to size and flight characteristics of European Odonata. *Odonatologica* **24**, 175–186.

HEGLUND, N. C. AND CAVANA, G. A. (1985). Efficiency of vertebrate locomotory muscles. *J. exp. Biol.* **115**, 283–292.

HEINRICH, B. (1993). *The Hot-Blooded Insects: Strategies and Mechanisms of Thermoregulation*. Cambridge, MA: Harvard University Press.

HEINRICH, B. AND CASEY, T. M. (1978). Heat transfer in dragonflies: 'fliers' and 'perchers'. *J. exp. Biol.* **74**, 17–36.

JENSEN, M. (1956). Biology and physics of locust flight. III. The

aerodynamics of locust flight. *Phil. Trans. R. Soc. Lond. B* **239**, 511–552.

JOSEPHSON, R. K. (1985). The mechanical power output of a tettigonid wing muscle during singing and flight. *J. exp. Biol.* **117**, 357–368.

JOSEPHSON, R. K. AND STEVENSON, R. D. (1991). The efficiency of a flight muscle from the locust *Schistocerca americana*. *J. Physiol., Lond.* **442**, 413–429.

LAN, C. E. (1979). The unsteady quasi-vortex-lattice method with applications to animal propulsion. *J. Fluid Mech.* **93**, 747–765.

LUTTGES, M. W. (1989). Accomplished insect fliers. In *Frontiers in Experimental Fluid Mechanics. Lecture Notes in Engineering 46* (ed. M. Gad-el-Hak), pp. 429–456. Berlin: Springer-Verlag.

MACHIN, K. E. AND PRINGLE, J. W. S. (1959). The physiology of insect fibrillar muscle. II. Mechanical properties of a beetle flight muscle. *Proc. R. Soc. Lond. B* **151**, 204–225.

MARDEN, J. H. (1987). Maximum lift production during takeoff in flying animals. *J. exp. Biol.* **130**, 235–258.

MARDEN, J. H. (1989). Bodybuilding dragonflies: costs and benefits maximising flight muscle. *Physiol. Zool.* **62**, 505–521.

MAY, M. L. (1976). Thermoregulation and adaptation to temperature in dragonflies (Odonata: Anisoptera). *Ecol. Monogr.* **46**, 1–32.

MAY, M. L. (1979). Energy metabolism of dragonflies (Odonata: Anisoptera) at rest and during endothermic warm-up. *J. exp. Biol.* **83**, 79–94.

MAY, M. L. (1982). Heat exchange and endothermy in Protodonata. *Evolution* **36**, 1051–1058.

MAY, M. L. (1995). Dependence of flight behaviour and heat production on air temperature in the green darner dragonfly, *Anax junius* (Odonata: Aeshnidae). *J. exp. Biol.* **198**, 2385–2392.

MIZISIN, A. P. AND JOSEPHSON, R. K. (1987). Mechanical power output of locust flight muscle. *J. comp. Physiol.* A **160**, 413–419.

NORBERG, R. Å. (1975). Hovering flight of the dragonfly *Aeschna juncea* L., kinematics and aerodynamics. In *Swimming and Flying in Nature*, vol. 2 (ed. T. Y. Wu, C. J. Brokaw and C. Brennen), pp. 763–781. New York: Plenum Press.

OSBORNE, M. F. M. (1951). Aerodynamics of flapping flight with application to insects. *J. exp. Biol.* **28**, 221–245.

PENNYCUICK, C. J. (1975). Mechanics of flight. In *Avian Biology*, vol. 5 (ed. D. S. Farner and J. R. King), pp. 1–75. London: Academic Press.

PENNYCUICK, C. J. AND REZENDE, M. A. (1984). The specific power output of aerobic muscle, related to the power density of mitochondria. *J. exp. Biol.* **108**, 377–392.

PFAU, H. K. (1986). Untersuchungen zur Konstruktion, Funktion und Evolution des Flugapparates der Libellen. *Tijdschr. Ent.* **129**, 35–123.

PFAU, H. K. (1991). Contributions of functional morphology to the phylogenetic systematics of Odonata. *Adv. Odonatol.* **5**, 109–141.

POLCYN, D. M. (1988). The thermal biology of desert dragonflies. PhD thesis. University of California, Riverside.

RÜPPELL, G. (1989). Kinematic analysis of symmetrical flight manoeuvres of Odonata. *J. exp. Biol.* **144**, 13–42.

SAHARON, D. AND LUTTGES, M. W. (1988). Visualisation of unsteady separated flow produced by mechanically driven dragonfly wing kinematics model. *AIAA Paper* no. 88-0569.

STEPNIEWSKI, W. Z. AND KEYS, C. N. (1984). *Rotary-wing aerodynamics*. New York: Dover.

STEVENSON, R. D. AND JOSEPHSON, R. K. (1990). Effects of operating frequency and temperature on mechanical power output from moth flight muscle. *J. exp. Biol.* **149**, 61–78.

SUNADA, S., KAWACHI, K., WATANABE, I. AND AZUMA, A. (1993). Performance of a butterfly in take-off flight. *J. exp. Biol.* **183**, 249–277.

VON MISES, R. (1959). *Theory of Flight*. New York: Dover.

WAINRIGHT, S. A., BIGGS, W. D., CURREY, J. D. AND GOSLINE, J. M. (1976). *Mechanical Design in Organisms*. London: Edward Arnold.

WAKELING, J. M. (1997). Odonatan wing and body morphologies. *Odonatologica* **26**, 35–52.

WAKELING, J. M. AND ELLINGTON, C. P. (1997*a*). Dragonfly flight. I. Gliding flight and steady-state aerodynamics. *J. exp. Biol.* **200**, 543–556.

WAKELING, J. M. AND ELLINGTON, C. P. (1997*b*). Dragonfly flight. II. Velocities, accelerations and kinematics of flapping flight. *J. exp. Biol.* **200**, 557–582.

WEIS-FOGH, T. (1960). A rubber-like protein in insect cuticle. *J. exp. Biol.* **37**, 889–907.

WEIS-FOGH, T. (1964). Biology and physics of locust flight. VIII. Lift and metabolic rate of flying locusts. *J. exp. Biol.* **41**, 257–271.

WEIS-FOGH, T. (1967). Respiration and tracheal ventilation in locusts and other flying insects. *J. exp. Biol.* **47**, 561–587.

WEIS-FOGH, T. (1972). Energetics of hovering flight in hummingbirds and *Drosophila*. *J. exp. Biol.* **56**, 79–104.

WEIS-FOGH, T. (1973). Quick estimates of flight fitness in hovering animals, including novel mechanisms for lift production. *J. exp. Biol.* **59**, 169–230.

WEIS-FOGH, T. AND ALEXANDER, R. MCN. (1977). The sustained power output from striated muscle. In *Scale Effects in Animal Locomotion* (ed. T. J. Pedley), pp. 511–525. London: Academic Press.

WILLMOTT, A. P. (1995). Mechanics of hawkmoth flight. PhD thesis. Cambridge University.

WOOTTON, R. J. (1974). The fossil record and insect flight. In *Insect Flight* (ed. R. C. Rainey), pp. 235–254. Oxford: Blackwell Scientific Publications.